nature medicine

Article

https://doi.org/10.1038/s41591-026-04491-7

Oligonucleotide–siRNA conjugate for SOD1 amyotrophic lateral sclerosis: a phase 1 trial

Received: 11 November 2025

Accepted: 28 May 2026

Published online: 15 July 2026

Check for updates

A list of authors and their affiliations appears at the end of the paper

Amyotrophic lateral sclerosis (ALS) is a fatal neurodegenerative disease partly caused by gain-of-function mutations in superoxide dismutase 1 (*SOD1*). Here we developed RAG-17, an siRNA-targeting *SOD1*, using an accessory oligonucleotide conjugate platform for enhanced central nervous system (CNS) delivery. Preclinically, RAG-17 rescued motor neuron degeneration, delayed disease progression, preserved motor function and extended survival in *SOD1*^{G93A} ALS rodents, even with advanced-stage treatment. In cynomolgus monkeys, intrathecal RAG-17 led to dose-dependent, durable reductions in *SOD1* mRNA (CNS) and protein (cerebrospinal fluid (CSF)). In a first-in-human trial in patients with *SOD1*-ALS ($n = 6$), participants were assigned to two cohorts—cohort 1 ($n = 3$) received an initial 60 mg dose (seven doses total) and cohort 2 ($n = 3$) received an initial 90 mg dose (six doses total). The dose was escalated in 30 mg steps to maintenance doses of 150 mg ($n = 5$) or 180 mg ($n = 1$). Thus, the primary safety endpoint was met, showing acceptable safety and tolerability. Treatment-emergent adverse events (TEAEs) occurred in 33% of participants (two of six). All TEAEs were mild to moderate, including muscle tremor (two patients) and elevated alanine aminotransferase (one patient), all of which resolved. No serious adverse events were reported. Furthermore, no other clinically meaningful changes were observed in laboratory parameters, vital signs, the ALS Functional Rating Scale-Revised score, physical or neurological examinations or ECG. The key secondary endpoints showed CSF SOD1 reductions of 69% (cohort 1, day 240) and 56% (cohort 2, day 210), and plasma neurofilament light chain reductions of 62% (cohort 1) and 52% (cohort 2), from baseline; no patient required invasive mechanical ventilation or died by the end of the study. These results demonstrate a favorable safety outcome, supporting the continued clinical evaluation of RAG-17 for *SOD1*-ALS. ClinicalTrials.gov registration: NCT05903690.

Amyotrophic lateral sclerosis (ALS) is a fatal neurodegenerative disease characterized by the progressive loss of motor neurons (MNs)[1]. Treatment options remain limited due to unclear pathogenesis[2]. Mutations in the superoxide dismutase 1 (*SOD1*) gene represent a key genetic cause, responsible for 15–30% familial ALS and up to 2% of all cases[3,4], with higher prevalence in Asian populations[5,6]. These mutations produce toxic misfolded SOD1 protein, thought to drive MN degeneration through a 'gain-of-function' mechanism[7–10]. Therefore, reducing mutant *SOD1* expression is a compelling therapeutic strategy for this subgroup.

This rationale led to accelerated approval of tofersen, an antisense oligonucleotide (ASO) that degrades *SOD1* mRNA, largely based on dramatic reduction of neurofilament light chain (NfL)[11]. In the phase 3 trial (VALOR), tofersen reduced plasma NfL levels and showed a significant difference in Amyotrophic Lateral Sclerosis Functional Rating Scale-Revised (ALSFRS-R) total scores between the early-treatment

e-mail: lilc@ractigen.com; yilong528@aliyun.com

and the delayed-treatment groups at 52 weeks[12]. Real-world evidence further suggests disease stabilization in some patients, with some benefits extending into the long-term treatment[13,14]. Single-stranded ASOs like tofersen leverage their self-delivering properties for cell entry[15]; other potent gene-silencing approaches are also under exploration.

Small interfering RNAs (siRNAs) offer potent and durable gene silencing through RNA interference (RNAi)[16,17], but effective delivery to the central nervous system (CNS) remains a major challenge[15]. Consequently, only a few siRNA programs have reached clinical development for CNS disorders, contrasting with multiple CNS-approved ASO drugs[15,18]. To address this, we developed a Smart Chemistry Aided Delivery (SCAD), which conjugates a therapeutic siRNA with an accessory oligonucleotide (ACO) to facilitate cellular uptake and tissue distribution, enabling the knockdown capabilities of the siRNA[19]. We previously reported that RAG-17 (a SCAD–siRNA also referred to as siSOD1-047M3-AC1^{VP}) demonstrated remarkable efficacy in *SOD1*^{G93A} mice[20].

In this study, we characterize the preclinical profile of RAG-17, including stability, specificity, pharmacokinetics (PK) and pharmacodynamics (PD) in rodents and nonhuman primates (NHPs). We then investigate its therapeutic efficacy in *SOD1*^{G93A} rats and mice. Finally, we report a human clinical trial assessing safety, tolerability, PK and preliminary efficacy in patients with *SOD1*-ALS, providing a comprehensive evaluation of RAG-17 from bench to bedside.

Results

In vitro stability, secondary pharmacology and immunogenicity analyses of RAG-17

RAG-17 is a therapeutic siRNA duplex against *SOD1* conjugated with a nontargeting, chemically modified ACO (Extended Data Fig. 1a). To characterize the preclinical profile of RAG-17, we first assessed its serum stability by incubating it with human serum for 24 h to 14 days (Extended Data Fig. 1b). Polyacrylamide gel electrophoresis analysis revealed that RAG-17 progressively released its duplex siRNA from day 1, while the ACO component remained mostly bound, indicating sufficient stability for tissue distribution and subsequent separation into oligonucleotides for cellular functions, supporting our hypothesis that ACO enhances the PK of SCAD (Extended Data Fig. 1c,d).

We then assessed the potential off-target genes of RAG-17 using in silico prediction followed by reverse transcription (RT)–qPCR in T98G cells 24 h post-transfection. Candidates were selected on the basis of perfect complementarity to the RAG-17 guide strand's 'seed' region and ≤4 mismatches in the extended region (Extended Data Fig. 1e). Five genes were identified—*CYTH2*, *NDUFC2*, *DISP2* and *KNOP1*, each of these genes containing three to four mismatches in their 3′ UTRs, and *UBAP2L*, which contains two mismatches in its coding region. RAG-17 did not significantly affect the mRNA levels of these genes at concentrations ranging from 0.25 nM to 25 nM (Extended Data Fig. 1e,f).

The immune stimulatory activity of RAG-17 was evaluated by an enzyme-linked immunosorbent assay (ELISA) using human peripheral blood mononuclear cells (PBMCs) treated with RAG-17 for 24 h through free uptake or RNAiMAX transfection. The assay also included the RAG-17 duplex and its ACO component. As shown in Extended Data Fig. 1g–l, neither RAG-17 itself nor its duplex or ACO components induced the expression of interferon (IFN)-α, tumor necrosis factor (TNF) or interleukin (IL)-1β.

Biodistribution and clearance of intrathecally administered RAG-17 in rodents

We performed RNAscope in situ hybridization (ISH) to assess the biodistribution of RAG-17. Assay specificity and quality were first validated using positive and negative control probes. A positive control probe (SR-RNU6-S1, hybridizing with U6 small nuclear 1 RNA) showed robust signal, whereas a negative control probe (SR-Scramble-S1, a scrambled sequence) showed no detectable signal in paraffin-embedded brain sections from vehicle (artificial cerebrospinal fluid (aCSF)) control rats (Extended Data Fig. 2). The assay revealed that RAG-17 is widely distributed throughout the rat CNS, with the highest concentrations in the lumbar spinal cord near the injection site (Extended Data Fig. 3a). Within the brain, the olfactory bulb, hippocampus and cerebellum exhibited higher levels of RAG-17 than other regions (Extended Data Fig. 3b). These results indicate that RAG-17 was effectively distributed to key CNS targets after intrathecal administration.

Liquid chromatography tandem–mass spectrometry analysis confirmed that RAG-17 levels were highest in the spinal cord, particularly in the lumbar region (Extended Data Fig. 3c,d). Levels were comparable across the brain stem, cerebellum, hippocampus and cerebrum, and were lowest in the striatum. CNS concentrations declined rapidly within the first 7 days and then stabilized thereafter, while liver and kidney concentrations declined rapidly and continuously over the same period (Extended Data Fig. 3e–h). Female rats exhibited slightly faster CNS clearance and slower kidney clearance than male rats (Extended Data Fig. 3e,h).

Among the peripheral tissues, the liver, kidney and spleen showed exposure levels comparable to those of CNS tissues, with the kidney being the highest (Extended Data Fig. 3c,d). However, the kidney and liver cleared faster (half-life, 6–9 days) than CNS tissues (half-life, 20–27 days; Extended Data Fig. 3e–h and Extended Data Table 1).

Postonset treatment with RAG-17 rescued muscle strength and extended the survival of *SOD1*^{G93A} mice

Building upon prior findings of presymptomatic efficacy[20], we investigated the therapeutic potential of RAG-17 when initiated well after symptom onset, a clinically relevant scenario. Female *SOD1*^{G93A} mice received two intracerebroventricular (ICV) doses of RAG-17 (200 µg or 400 µg) or vehicle (aCSF) on postnatal days (PNDs) 126 and 151 (Fig. 1a). This timing is significantly later than the typical symptom onset (around PNDs 90–100) in this model[21,22] and contrasts with most preclinical ALS studies that initiate treatment earlier[23,24].

Strikingly, even with this delayed administration, RAG-17 yielded substantial therapeutic benefits. Both low (200 µg) and high (400 µg) doses improved motor performance (Fig. 1b), muscle strength (Fig. 1c) and body weight versus controls (Fig. 1d), often dose dependently. Relative to controls (median survival—169.5 days), late administration of RAG-17 at 200 and 400 µg delayed disease progression by 1 day and 45.5 days, and extended survival by 78.5 days (46.3% increase) and 128.5 days (75.8% increase), respectively (Fig. 1e–g). While early treatment (PND 70/100) produced the most profound lifespan extension (median 331 days, 95% increase), these data demonstrate that RAG-17 retains substantial efficacy even when administered late in disease progression.

RAG-17 delayed disease onset, extended survival and improved motor function in *SOD1*^{G93A} ALS rats

To evaluate repeat-dose efficacy, *SOD1*^{G93A} rats received two intrathecal injections of 0.9 mg RAG-17 ($n = 16$) or nontargeting control (NTC; $n = 20$) on PNDs 70 and 130; wild-type (WT) controls received aCSF ($n = 11$). RAG-17 markedly delayed disease onset (neurological score = 1). NTC rats exhibited a median onset of 187.5 days and median lifespan of 215.5 days, whereas the RAG-17 group did not reach median onset by the 290-day study endpoint (Extended Data Fig. 4a), with only 1 of 16 rats developing symptoms. RAG-17-treated rats maintained body weight (Extended Data Fig. 4b), muscle strength (Extended Data Fig. 4c), motor function (Extended Data Fig. 4d), delayed paralysis (Extended Data Fig. 4e) and extended survival (Extended Data Fig. 4f). Choline acetyltransferase (ChAT) staining of the lumbar spinal cord revealed that RAG-17 significantly preserved MNs compared to NTC (42.2% increase, $P = 0.0409$), but not to WT levels (Extended Data Fig. 4g–j). The robust functional benefits, despite incomplete MN rescue at this late disease stage, suggest that RAG-17

https://doi.org/10.1038/s41591-026-04491-7

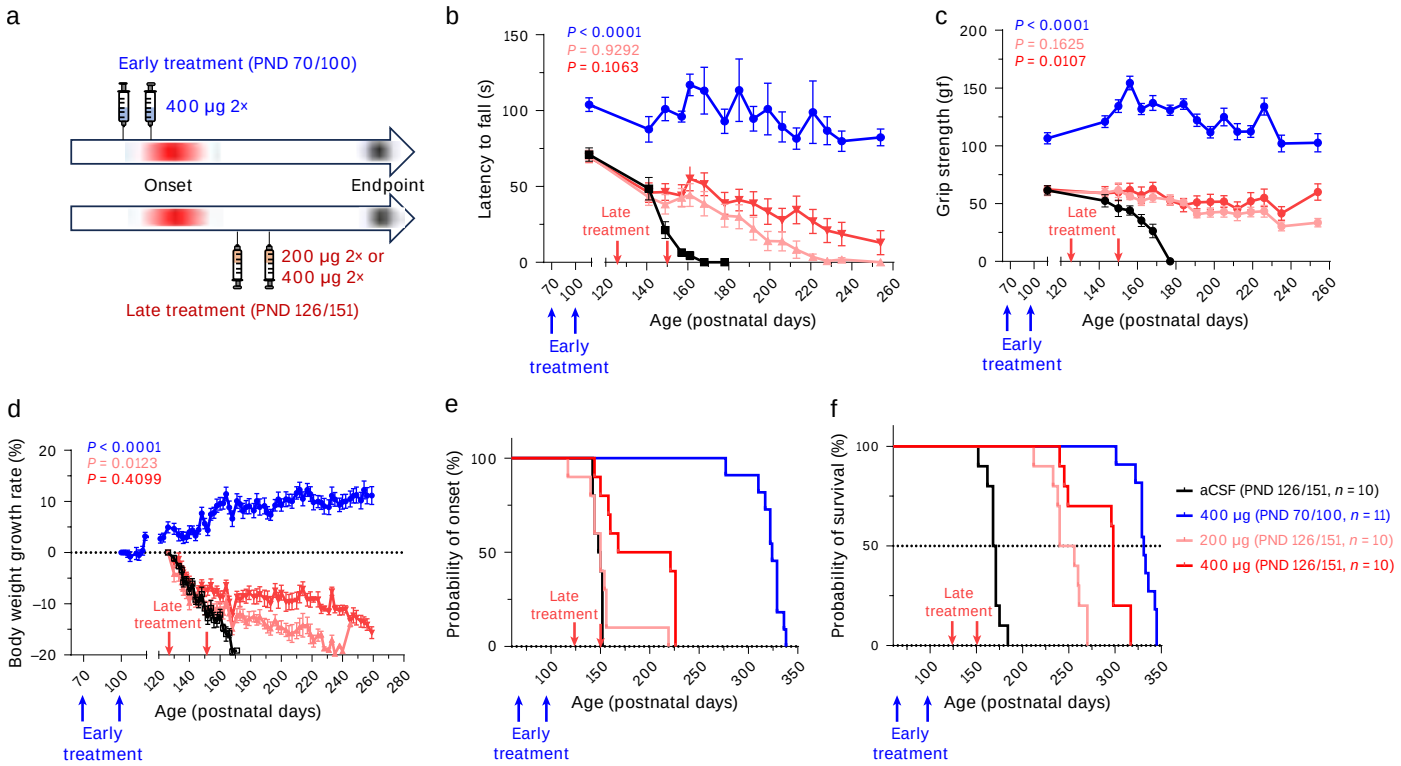

g

Group	aCSF (@PND 126/151)	Early-400 µg (@PND 70/100)	Late-200 µg (@PND 126/151)	Late-400 µg (@PND 126/151)
Number of animals	10	11	10	10
Median onset (days)	149	324 ($P < 0.0001$)	150 ($P = 0.2624$)	194.5 ($P = 0.0008$)
Delayed onset (days)		175	1	45.5
Median survival (days)	169.5	331 ($P < 0.0001$)	248 ($P < 0.0001$)	298 ($P < 0.0001$)
Extended lifespan (days)		161.5	78	128

Fig. 1 | Therapeutic efficacy of early or late administration of RAG-17 in *SOD1*^{G93A} mice. a, Schematic of the study design for early or late treatment in female *SOD1*^{G93A} mice. ICV injections were administered as follows: aCSF ($n = 10$) on PNDs 126 and 151, early RAG-17 ($n = 11$, 400 µg) on PNDs 70 and 100, late-low RAG-17 ($n = 10$, 200 µg) on PNDs 126 and 151 and late-high RAG-17 ($n = 10$, 400 µg) on PNDs 126 and 151. **b**–**d**, Motor function assessed by the rotarod test (**b**), forelimb muscle grip strength (**c**) and body weight change (%) (**d**). Data are presented as mean ± s.e.m. Initial sample sizes were $n = 10$ (aCSF), $n = 11$ (early-treatment 400 µg), $n = 10$ (late-treatment 200 µg) and $n = 10$ (late-treatment 400 µg). Sample sizes for each group decreased over time as animals reached their humane endpoint. Statistical significance was determined by one-way ANOVA with Dunnett's multiple comparisons test compared with the aCSF control. *P* values are color-coded by treatment group—blue indicates early treatment; light and dark red indicate 200 µg and 400 µg late-treatment, respectively. **e**, Disease onset defined as a 10% loss of body weight from peak body weight. **f**, Kaplan–Meier survival curves. **g**, Summary of disease onset and survival data from **e** and **f**. Statistical significance for **e** and **f** was determined by the log-rank (Mantel–Cox) test compared to the aCSF group.

facilitates functional compensation by preserving motor units, underscoring its disease-modifying potential.

RAG-17 exhibits potent and durable CNS SOD1 knockdown in cynomolgus monkeys

We confirmed RAG-17 activity in cynomolgus monkeys despite a single-nucleotide mismatch at position 13 (from the 5′ end) of its antisense strand relative to cynomolgus *SOD1* mRNA. RAG-17 effectively knocked down *SOD1* in COS-1 cells (derived from African green monkeys), which share an identical target of *SOD1* sequence with cynomolgus monkeys, with efficiency comparable to that in human T98G cells (Extended Data Fig. 5a). These findings suggest that this single mismatch does not substantially compromise RAG-17 activity, supporting the use of cynomolgus monkeys for PD studies.

After intrathecal administration in cynomolgus monkeys, RAG-17 demonstrated dose-dependent exposure in both CSF and plasma (Extended Data Fig. 5b). CSF levels were substantially higher than plasma levels, with CSF-to-plasma ratios ranging from 200 to 900 between 2 and 48 h postdose. Peak CSF concentrations occurred within 15 min and declined rapidly within 48 h. In contrast, plasma concentrations peaked at 2–4 h and declined more slowly. This PK profile indicates rapid CSF distribution followed by drainage into plasma, confirming intrathecal administration as an effective CNS-targeting route with minimal systemic exposure.

PD analysis of NHP tissue samples revealed that RAG-17 dose dependently reduced *SOD1* mRNA and protein levels across CNS tissues and in the CSF (Fig. 2a–g). Notably, the 50 mg dose achieved a 91% reduction in *SOD1* mRNA in the lumbar spinal cord, an effect that persisted for up to 72 days. In the cerebral cortex, distal to the injection site, peak knockdown activity was 40% at 20 mg and exceeded 70% at 50 mg. These mRNA reductions correlated with decreased SOD1 protein levels in the CSF.

Integrated PK/PD analysis of the cynomolgus monkey data confirmed robust, dose-dependent on-target effects. The estimated

effective dose for 50% inhibition (ED_{50}) in the lumbosacral spinal cord was 3.889 mg and 5.031 mg on days 22 and 71, respectively (Fig. 2h). In the cerebral cortex, calculated ED_{50} values were 51.37 mg and 108.4 mg for the same time points (Fig. 2k). Notably, *SOD1* knockdown activity exhibited a strong correlation with RAG-17 tissue exposure across all groups (Fig. 2i,l). Based on a three-parameter logistic sigmoidal model, the half-maximal inhibitory concentrations IC_{50} were determined to be 165.2 ng g^{-1} in the lumbosacral spinal cord and 376.1 ng g^{-1} in the cerebral cortex (Fig. 2j,m). These findings provide a quantitative framework for predicting PD responses and for guiding dose selection for patients with ALS.

Design of the human clinical trial, participant disposition and baseline characteristics

In this open-label, single-center, dose-escalation trial, adults with *SOD1*-ALS received multiple intrathecal RAG-17 doses to evaluate safety, tolerability, PK and PD. The trial design is schematically illustrated in Fig. 3a, with further protocol details available in Methods and Supplementary Data—Protocol.

Between 22 May 2023 and 27 November 2023, seven individuals were screened and six were enrolled (one excluded for low forced vital capacity (FVC)). They were assigned to two cohorts—cohort 1 ($n = 3$) received an initial RAG-17 dose of 60 mg (seven total doses), while cohort 2 ($n = 3$) received an initial 90 mg dose (six total doses; Fig. 3a,b). Doses escalated by 30-mg increments to maintenance of 150 mg ($n = 5$) or 180 mg ($n = 1$). All six participants completed treatment and study visits (final visit on 11 July 2024).

The six participants (age = 26–67 years, four females) all carried out a confirmed pathogenic or likely pathogenic *SOD1* mutation; four reported a family history. One harbored the p.Gly142Ala variant, historically of conflicting pathogenicity interpretations, but now supported as pathogenic by the absence from gnomAD, published cases[25,26], and in silico modeling (indicating a 95% probability of disrupting *SOD1* function; ClinVar ID—2436219). Consequently, this participant was included in the study. Detailed baseline characteristics, including body mass index, ALSFRS-R score, percentage of FVC (%) and plasma NfL levels, are summarized in Table 1.

Primary outcomes (safety) of the human clinical trial

RAG-17 was generally well tolerated, with no serious adverse events (SAEs) up to the data cutoff. TEAEs are provided in Table 2.

TEAEs occurred in two of six participants (33%). Cases 1 and 2 experienced transient, mild muscle tremors after their initial RAG-17 doses (60 mg and 90 mg, respectively), resolving spontaneously without recurrence upon escalation. These events were considered treatment related. Separately, case 1 (pre-existing fatty liver and abnormal liver function) had asymptomatic alanine aminotransferase (ALT) elevation (to >1.5 times baseline) before the 180 mg dose; the treatment continued with no further ALT rise. This event was assessed as potentially related to both RAG-17 and the underlying condition. Other AEs included headache ($n = 2$ incidents), falls ($n = 2$), cold (n = 1), fever ($n = 1$), abdominal pain ($n = 1$), urinary tract infection ($n = 1$) and pain in extremities ($n = 1$). The headaches were positional, resolved with intravenous hydration and were assessed as postdural puncture headaches related to the procedure, but not to RAG-17. All other AEs were considered unrelated to the study drug, consistent with intercurrent illnesses or ALS progression.

Other than the ALT elevation in case 1, no clinically meaningful changes were observed in other laboratory parameters, including complete blood count (Supplementary Tables 1–18) and basic metabolic panel (Supplementary Tables 19–58). No notable abnormalities were found in continuous vital signs (blood pressure, heart rate, respiratory rate, temperature) during hospitalization (Supplementary Tables 59–62), physical examinations (cardiac, pulmonary, abdominal), neurological examination (Supplementary Tables 63–66) or electrocardiograms (ECG) findings (Supplementary Table 67). Additionally, two exploratory post hoc analyses were performed. First, body weight changes from baseline over 240 days were variable—one patient (case 3) showed a transient 15% peak increase before returning to baseline by day 120; the other five remained within ±5% of baseline (Extended Data Table 2). Second, serial CSF protein concentrations (Supplementary Table 68) showed individual fluctuations without clinical symptoms of radiculitis or myelitis. Notably, systematic serial CSF cell count analysis was not performed; therefore, correlation with subclinical pleocytosis cannot be assessed.

ALSFRS-R scores over up to 210 of 240 days showed individual fluctuations (Fig. 3c). Case 3 improved four-point scale at the final visit; case 2 had the greatest decline, primarily driven by respiratory subscores. The pretreatment progression rate was estimated based on the decline in ALSFRS-R score relative to disease duration before baseline. The overall pretreatment rate was estimated at 0.430 ± 0.172 points per month. After treatment, the observed progression rate was 0.295 ± 0.187 points per month (Supplementary Table 69). Further exploratory post hoc analysis revealed distinct patterns based on baseline disease severity and duration. Patients with higher baseline scores of >40 (cases 1, 2 and 6) had a lower pretreatment progression rate (0.127 ± 0.036 points per month), but increased post-treatment to 0.423 ± 0.177 points per month (exceeding individual pretreatment rates in cases 1 and 2), possibly reflecting natural variability or a floor effect. In contrast, participants with intermediate baseline scores (between 30 and 40; cases 3 and 5) had a higher pretreatment progression rate (0.838 ± 0.362 points per month) and demonstrated deceleration after treatment (−0.107 ± 0.393 points per month). The patient with the lowest score <30 (case 4) had modest acceleration post-treatment (0.714 versus 0.523 points per month). Post-treatment progression rates appeared more favorable in patients with shorter disease duration (≤21 months) than in those with longer disease duration (≥36 months), suggesting distinct subgroups with different baseline characteristics and potential differential responses. For most participants, ALSFRS-R subdomains (bulbar, trunk, upper limb and lower limb functions) showed no substantial change throughout the study period (Extended Data Fig. 6a–d), whereas respiratory function scores (Extended Data Fig. 6e) gradually declined in some patients, reflecting heterogeneity in disease progression.

Secondary outcomes of the human clinical trial

PK analysis was conducted after each dose. Generally, plasma RAG-17 concentrations typically peaked 6–12 h after intrathecal injection, and returned to near baseline by 48 h postdose (Fig. 3d–j). However, atypical PK profiles were noted at specific time points in two participants. Case 4 showed an unexpectedly early peak (1 h) after the second dose and had levels below the lower limit of quantification after the sixth dose (Fig. 3h). Case 5 exhibited rapid peaks within 4 h after the first and fourth doses (Fig. 3i). These sporadic, early peaks with the direct entry of a small fraction of the administered dose into the systemic circulation during or immediately after lumbar puncture are observed. Potential contributing factors include (1) procedural variability in lumbar puncture, such as needle tip position, injection pressure or CSF reflux, which could facilitate direct vascular exposure; and (2) individual anatomical and physiological differences, such as variations in spinal venous drainage or CSF dynamics, which may influence drug redistribution from the CSF compartment. Despite this variability, robust CSF SOD1 reductions were consistently observed, indicating that central PD activity is driven by local CSF exposure and remains effective regardless of peripheral PK fluctuations.

PD markers indicated robust target engagement after RAG-17 administration. CSF SOD1 protein levels decreased progressively and substantially in all participants with repeated dosing (Fig. 3k and Extended Data Fig. 6f). Compared to baseline, the mean reduction was

https://doi.org/10.1038/s41591-026-04491-7

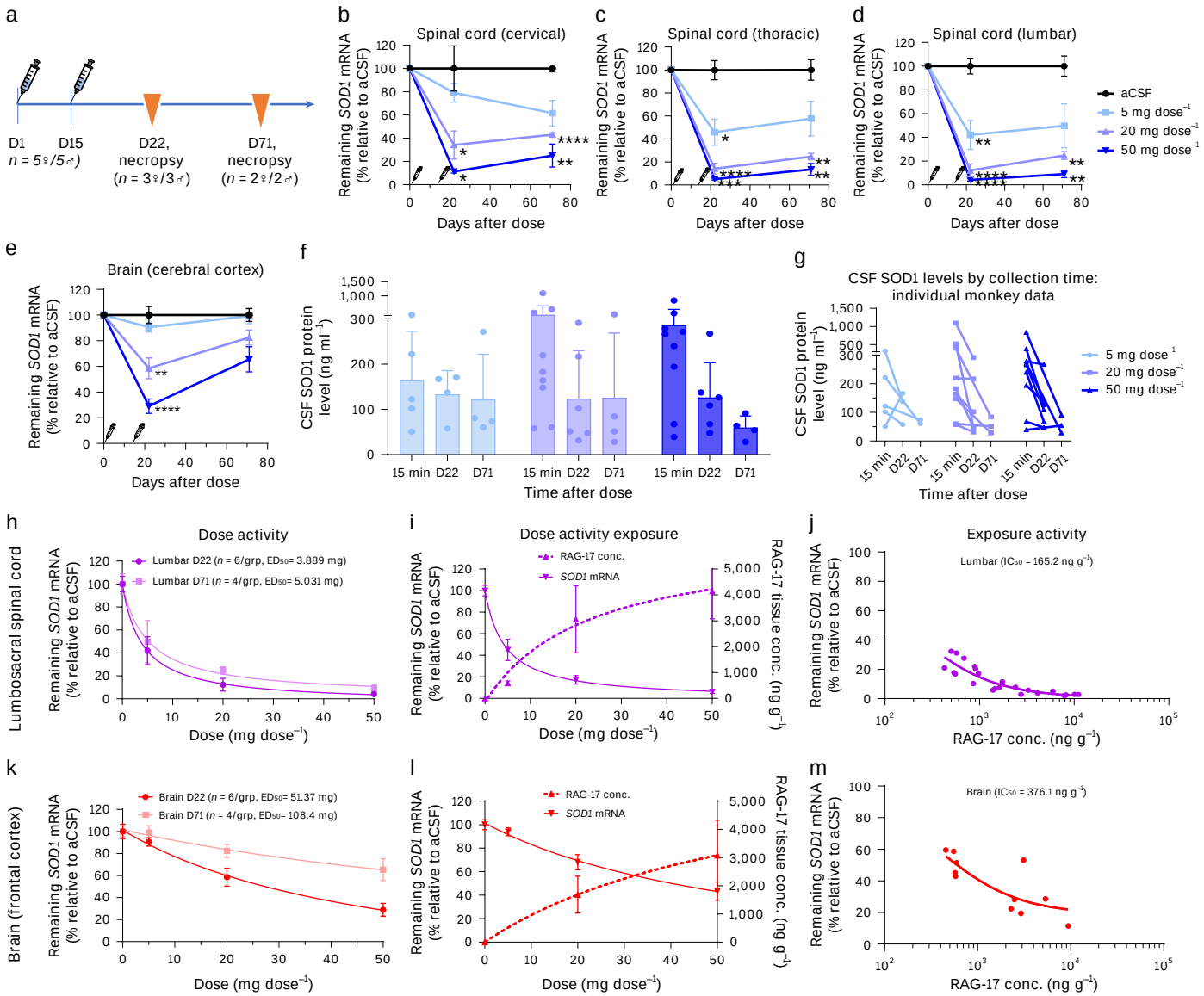

Fig. 2 | Translational PD of RAG-17 in cynomolgus monkeys. Monkeys received two intrathecal injections of either aCSF or RAG-17 (5, 20 or 50 mg per dose) on day 1 and day 15, followed by necropsies for histopathological and pharmacological analysis at the indicated time points. **a**, Schematic of the study design showing the two intrathecal doses and scheduled necropsies ($n = 6$ for day 22; $n = 4$ for day 71). **b**–**e**, *SOD1* mRNA levels quantified by RT–qPCR and expressed as a percentage of the remaining *SOD1* mRNA relative to the aCSF control group in the cervical (**b**), thoracic (**c**) and lumbar (**d**) spinal cord regions and the cerebral cortex (**e**) brain region. Data are presented as mean ± s.e.m. ($n = 6$ per group on day 22; $n = 4$ per group on day 71). **f**,**g**, CSF SOD1 protein levels assessed by ELISA. **f**, Data are presented as mean ± s.d. with individual data points overlaid for each group at baseline (predose, $n = 6$), day 22 ($n = 6$) and day 71 ($n = 4$) after the first dose. **g**, Individual trajectories of CSF SOD1 protein levels for each monkey across all time points. **h**,**k**, Dose-dependent *SOD1* mRNA knockdown in the lumbosacral spinal cord (**h**) and frontal cortex (**k**) at days 22 and 71. Data are presented as mean ± s.e.m. ($n = 6$ per group for day 22; $n = 4$ per group for day 71). **i**,**l**, Comparison of RAG-17 tissue exposure (right, *y* axis) and *SOD1* mRNA silencing (left, *y* axis) across doses in the spinal cord (**i**) and brain (**l**), combining data from days 22 and 71. Data are presented as mean ± s.e.m. **j**,**m**, Exposure–response correlation plots showing *SOD1* mRNA levels versus tissue concentration in the spinal cord (**j**) and brain (**m**). Samples with tissue concentrations below the limit of quantification were excluded, resulting in $n = 23$ (**j**) and $n = 11$ (**m**) data points. *P* values were determined by one-way ANOVA followed by Dunnett's multiple comparisons test. *$P < 0.05$; **$P < 0.01$; ***$P < 0.001$; ****$P < 0.0001$. Conc., concentration; grp, group.

69% on day 240 in cohort 1 ($n = 3$, seven doses) and 56% on day 210 in cohort 2 ($n = 3$, six doses).

Plasma NfL, a marker of neuroaxonal injury, decreased after treatment initiation (Fig. 3l). Five of six participants achieved robust reductions (individual nadirs—approximately 50–85% from baseline). Case 1 exhibited an initial decrease of over 60% by day 120, followed by a rebound to near baseline by day 240, differing from the sustained decline characteristic in the other five; thus, case 1 was excluded from the aggregated longitudinal analysis presented in Extended Data Fig. 6g. At study end, mean plasma NfL reduction relative to baseline was 62% at day 240 for cohort 1 and 52% at day 210 for cohort 2 (Extended Data Fig. 6g). The nadir occurred before the maintenance phase (after the fifth dose), followed by a slight increase during the longer dosing intervals; however, levels remained well below the baseline for all participants at the end. The largest reductions were in participants with higher baseline NfL. In an exploratory post hoc CSF analysis, NfL kinetic profile mirrored plasma changes, showing an initial decline after treatment initiation and a modest rebound during

https://doi.org/10.1038/s41591-026-04491-7

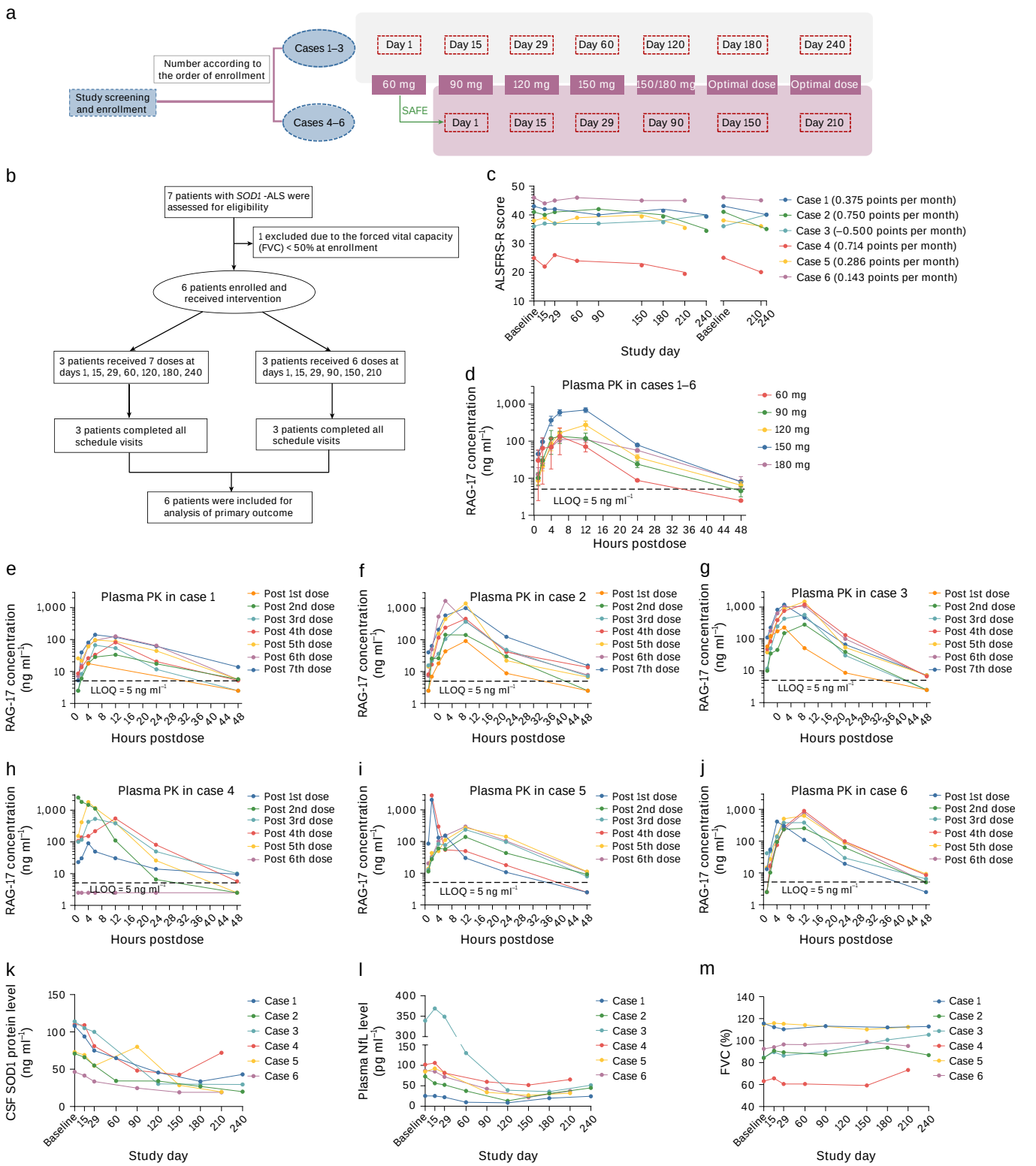

Fig. 3 | Design of the clinical trial and patient outcomes. a, Design of the dose-escalation study of RAG-17. The first three participants received an initial intrathecal injection of 60 mg, while the subsequent three participants started at a dose of 90 mg. RAG-17 was administered through intrathecal injection with escalating doses (60, 90, 120, 150 mg), culminating in a final maintenance dose of 150/180 mg^{-1} (capped at 180 mg). The last two administrations represented the optimal dose levels. **b**, Participant flow diagram. **c**, Longitudinal changes in total ALSFRS-R score for each patient. **d**, Aggregate plasma PK of RAG-17 across different dose levels for all patients. Bars represent mean ± s.e.m.; individual data points (dots) are overlaid. For each dose level, the exact number of PK sample observations (n) is as follows: 60 mg ($n = 3$ samples), 90 mg ($n = 5$ samples), 120 mg ($n = 7$ samples), 150 mg ($n = 17$ samples) and 180 mg ($n = 3$ samples). Specific anomalous PK values were excluded from the analysis (case 4, second and sixth doses; case 5, first and fourth doses). **e**–**j**, Individual plasma PK profiles of RAG-17 for each participant after each dose administration—case 1 (**e**), case 2 (**f**), case 3 (**g**), case 4 (**h**), case 5 (**i**) and case 6 (**j**). **k**, CSF SOD1 protein levels presented as individual patient trajectories. **l**, Plasma NfL levels presented as individual patient trajectories. **m**, Longitudinal changes of FVC for each patient. The horizontal dashed line in the background (**d**–**j**) represents the lower limit of quantification (LLOQ) of RAG-17.

Table 1 | Baseline demographic and clinical characteristics

Baseline characteristics	All (*n* = 6)	Case 1 (Pt 0001)	Case 2 (Pt 0002)	Case 3 (Pt 0003)	Case 4 (Pt 0005)	Case 5 (Pt 0006)	Case 6 (Pt 0007)
Demographics							
Age (years)	45.5±15.3	31	26	44	67	55	50
Sex, female, *n* (%)	4 (66.7)	Male	Female	Female	Female	Female	Male
BMI (kg m^{-2})	23.3±6.9	35.9	16.6	17.8	23.4	24.3	21.7
Disease duration (months)	33.3±22.7	72	36	10	44	21	17
Family history	4 (66.7)	Yes	Yes	No	Yes	Yes	No
SOD1 mutation							
p.Gly42Asp, *n* (%)	2 (33.3)	Yes	–	Yes	–	–	–
p.Asn87Ser, *n* (%)	1 (16.7)	–	Yes	–	–	–	–
p.Gly142Ala, *n* (%)	1 (16.7)	–	–	–	Yes	–	–
p.Ser106Leu, *n* (%)	1 (16.7)	–	–	–	–	Yes	–
p.His49Arg, *n* (%)	1 (16.7)	–	–	–	–	–	Yes
Previous treatment history							
Riluzole use, *n* (%)	4 (66.7%)	Yes	No	Yes	Yes	Yes	No
Edaravone use, *n* (%)	1 (16.7%)	No	No	Yes	No	No	No
Laboratory values							
Plasma NfL (pg ml^{-1})	118.5±111.2	25.3	72.9	339	102	84.9	87.0
CSF SOD1 (ng ml^{-1})	87.0±27.6	108	70.9	114	110	72.9	46.4
Clinical assessment							
ALSFRS-R	38.2±7.4	43	41	36	25	38	46
FVC (%)	92.5±20.1	115.6	84.2	84.7	63.1	114.8	92.5

Summary data for the six patients (including age, BMI, disease duration, plasma NfL, CSF SOD1, ALSFRS-R and FVC) are presented as mean±s.d. Disease duration is measured from the reported date of symptom onset. BMI, body mass index.

Table 2 | Summary of AEs

Dosage (mg dose^{-1})	60 (*n*=3)	90 (*n*=6)	120 (*n*=6)	150 (*n*=5)	180 (*n*=1)
Tremor muscle	1 (33%; possibly related)	1 (17%; possibly related)	0	0	0
Headache	1 (33%; probably unrelated)	0	1 (17%; probably unrelated)	0	0
Cold	1 (33%; definitely unrelated)	0	–	0	0
Fever	0	0	1 (17%; probably unrelated)	0	0
Abdominal pain	1 (33%; probably unrelated)	0	–	0	0
Urinary tract infection	0	0	1 (17%; probably unrelated)	0	0
Elevated ALT	0	0	1 (17%; possibly related)	0	0
Fall	0	0	1 (17%; definitely unrelated)	0	1 (100%; definitely unrelated)
Pain in extremity	0	0	0	1 (20%; definitely unrelated)	0

the extended-interval maintenance phase (Supplementary Table 70). This concordance strengthens that the observed NfL reductions reflect a true treatment effect on neuronal integrity, and supports the use of plasma NfL as a practical and responsive biomarker in this setting.

No patient required invasive mechanical ventilation or died.

Exploratory outcomes of the human clinical trial

Among the six participants, exploratory outcome measures showed variability. Lung function, assessed by percent predicted FVC (%FVC), showed delayed deterioration in most participants. Cases 3 and 4 exhibited improvement over their baseline %FVC values by the end of the study (Fig. 3m). Muscle strength assessments indicated no marked decline in most participants, with some measures showing improvement (Supplementary Tables 71–85). Quality of life and functional scales (the modified Norris scale, Amyotrophic Lateral Sclerosis Assessment Questionnaire 40 (ALSAQ-40) and the five-level version of EuroQol Five Dimensions Questionnaire (EQ-5D-5L)) showed slight declines (Fig. 4a–c), while measures of anxiety (Hamilton Anxiety Rating Scale (HAMA)), depression (Hamilton Depression Rating Scale (HAMD)) and fatigue (Fatigue Severity Scale (FSS)) showed little change (Fig. 4d–f). Electromyography parameters (composite muscle action potentials and motor unit number index) changed slowly, whereas motor unit size

https://doi.org/10.1038/s41591-026-04491-7

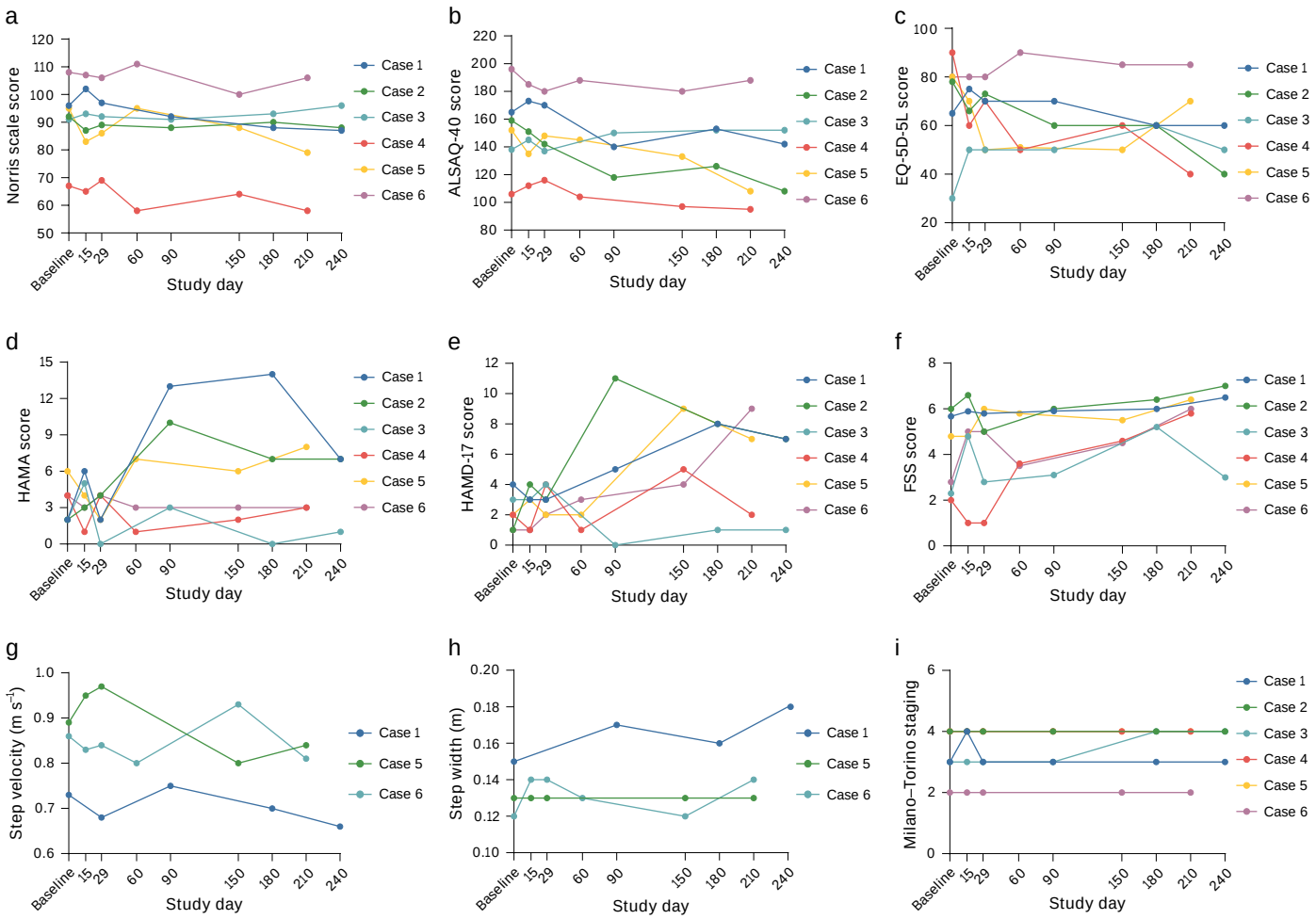

Fig. 4 | Exploratory outcomes of RAG-17 in patients. a–i, Longitudinal changes in clinical outcome for individual patients—Norris scale scores (**a**), ALSAQ-40 scores (**b**), EQ-5D-5L scores (**c**), HAMA scores (**d**), HAMD scores (**e**), FSS score (**f**), gait function assessed by three-dimensional gait analysis under multitasks (including step velocity (**g**), step width (**h**)) and Milano–Torino staging (**i**).

index showed a gradual increase (Supplementary Tables 86–94). Gait function exhibited minimal changes or a gradual decline (Fig. 4g,h, Extended Data Fig. 6h,i and Supplementary Tables 95–101). Clinical staging remained unchanged in four participants, while two participants experienced progression (Supplementary Table 102 and Fig. 4i). Baseline 7 T MRI SWI revealed the presence of the motor band sign (iron deposition in the precentral gyrus) in three of six enrolled participants. In all participants, this neuroimaging signature showed no appreciable change over the course of the study, as assessed at post-treatment days 29, 90, 180 and 240.

Discussion

This study presents a comprehensive evaluation of RAG-17, a siRNA–ACO conjugate targeting *SOD1*, developed using the SCAD delivery platform. Our findings include in vitro characterization, preclinical assessments in rodent models and NHPs, and a human clinical trial in *SOD1*-ALS. The data support RAG-17 as a therapeutic candidate for *SOD1*-ALS, a disease with limited effective treatments. While the approval of the ASO tofersen was a landmark achievement, alternative strategies with potentially improved safety and dosing profiles are still needed[27].

A formidable challenge in RNAi therapeutics is CNS delivery[15]. The SCAD platform enables functional siRNA delivery across multiple CNS cell types, achieving sustained *SOD1* knockdown in NHPs, with mRNA reduction persisting up to 71 days, suggesting a potential for less frequent intrathecal dosing. Reference 28 discussed durable *SOD1* reduction for up to 100 days after the final ASO administration in NHPs. Together, these findings suggest that extended dosing intervals may be achievable with RAG-17, warranting clinical evaluation. In the aggressive *SOD1*^{G93A} mouse model, RAG-17 administered at a very late disease stage (PNDs 126 and 151) showed striking efficacy[23]. Previous interventions initiated after symptom onset typically began before PND 90 and reported modest survival benefits[29–31]. Late-stage RAG-17 treatment produced unprecedented survival and functional benefits, suggesting potential for advanced or rapidly progressing disease.

Our data demonstrate target engagement and pharmacological activity. Intrathecal administration of RAG-17 reduced CSF SOD1 protein and plasma NfL levels, within the range reported for tofersen in *SOD1*-ALS[12]. These biomarker changes coincided with preliminary clinical signals. Natural history studies report variable progression rates in *SOD1*-ALS depending on the specific mutation, with some variants (for example, A4V) associated with rapid decline[5,32]. Cross-trial comparisons are limited by differences in design, populations and outcome measures. Direct comparisons should be cautious given substantial differences—the cited tofersen trials enriched faster-progressing variants, while many variants in this study have slower natural history progression[12,33,34].

In this small cohort, RAG-17 demonstrated a favorable safety and tolerability profile. We did not observe clinical signs of inflammatory responses or neurotoxic AEs as reported with some ASOs, such as tofersen[13]. One possible explanation is that the shorter oligonucleotide length of RAG-17 (specifically, its 14-nucleotide ACO component,

which is notably shorter than tofersen's 20-nucleotide ASO) may be less prone to trigger the off-target hybridization or innate immune pathway activation commonly implicated in ASO-related toxicities[35]. Direct comparative safety assessments will require larger, controlled trials.

The clinical translation of the SCAD platform, demonstrating functional siRNA delivery and a robust PD effect in the human CNS, marks a key milestone for oligonucleotide therapeutics. This achievement validates the SCAD as a platform to overcome siRNA delivery challenges, potentially enabling RNAi therapies for other neurological targets.

Limitations of this study include the open-label design, small sample size and retrospectively estimated pretreatment progression rates (lacking prospective ALSFRS-R data), which limit the precision in quantifying treatment effect. Heterogeneity of *SOD1* mutations, with some having slower natural history progression, limits comparisons with external cohorts. Additionally, the absence of serial CSF cell data in both the human and animal studies means that potential subclinical inflammatory responses cannot be excluded. While CSF protein data are available, they provide only partial insight into potential inflammatory responses at the cellular level. Limited tissue availability from the completed preclinical studies prevented neuromuscular junction (NMJ) denervation assessments, which could have provided further insight into the efficacy of RAG-17. In particular, NMJ denervation status would have complemented the functional and biomarker data. Longer-term observation and larger, randomized controlled trials are necessary to establish the safety and efficacy. Future studies should incorporate CSF profiling, including cell counts, a pretreatment observation period for reliable baseline progression and histopathological evaluations such as NMJ analyses. Nonetheless, consistent preclinical efficacy, robust biomarker responses and preliminary clinical signals support continued development.

In conclusion, RAG-17, a SCAD-delivered siRNA, demonstrates robust SOD1 silencing and efficacy in preclinical models. In its human clinical trial, it met the primary endpoint of favorable safety and tolerability across tested doses. RAG-17 provides an additional therapeutic option for *SOD1*-ALS and validates the SCAD platform for the next generation of RNAi therapies in neurological diseases.

Online content

Any methods, additional references, Nature Portfolio reporting summaries, source data, extended data, supplementary information, acknowledgements, peer review information; details of author contributions and competing interests; and statements of data and code availability are available at https://doi.org/10.1038/s41591-026-04491-7.

References

1. Feldman, E. L. et al. Amyotrophic lateral sclerosis. *Lancet* **400**, 1363–1380 (2022).
2. Al-Khayri, J. M. et al. Amyotrophic lateral sclerosis: insights and new prospects in disease pathophysiology, biomarkers and therapies. *Pharmaceuticals* **17**, 1391 (2024).
3. Rosen, D. R. et al. Mutations in Cu/Zn superoxide dismutase gene are associated with familial amyotrophic lateral sclerosis. *Nature* **362**, 59–62 (1993).
4. Zou, Z. Y. et al. Genetic epidemiology of amyotrophic lateral sclerosis: a systematic review and meta-analysis. *J. Neurol. Neurosurg. Psychiatry* **88**, 540–549 (2017).
5. Chen, L. X. et al. *SOD1* mutation spectrum and natural history of ALS patients in a 15-year cohort in Southeastern China. *Front. Genet.* **12**, 746060 (2021).
6. Liu, Z. et al. Mutation spectrum of amyotrophic lateral sclerosis in Central South China. *Neurobiol. Aging* **107**, 181–188 (2021).
7. Ilieva, H. S. et al. Mutant dynein (Loa) triggers proprioceptive axon loss that extends survival only in the SOD1 ALS model with highest motor neuron death. *Proc. Natl Acad. Sci. USA* **105**, 12599–12604 (2008).
8. Bruijn, L. I. et al. Aggregation and motor neuron toxicity of an ALS-linked SOD1 mutant independent from wild-type SOD1. *Science* **281**, 1851–1854 (1998).
9. Brown, R. H. Jr. Superoxide dismutase in familial amyotrophic lateral sclerosis: models for gain of function. *Curr. Opin. Neurobiol.* **5**, 841–846 (1995).
10. Sau, D. et al. Mutation of SOD1 in ALS: a gain of a loss of function. *Hum. Mol. Genet.* **16**, 1604–1618 (2007).
11. Blair, H. A. Tofersen: first approval. *Drugs* **83**, 1039–1043 (2023).
12. Miller, T. M. et al. Trial of antisense oligonucleotide tofersen for *SOD1* ALS. *N. Engl. J. Med.* **387**, 1099–1110 (2022).
13. Smith, S. E. et al. Tofersen treatment leads to sustained stabilization of disease in SOD1 ALS in a 'real-world' setting. *Ann. Clin. Transl. Neurol.* **12**, 311–319 (2025).
14. Sabatelli, M. et al. Long-term treatment of SOD1 ALS with tofersen: a multicentre experience in 17 patients. *J. Neurol.* **271**, 5177–5186 (2024).
15. Goto, A., Yamamoto, S. & Iwasaki, S. Biodistribution and delivery of oligonucleotide therapeutics to the central nervous system: advances, challenges, and future perspectives. *Biopharm. Drug Dispos.* **44**, 26–47 (2023).
16. Elbashir, S. M., Lendeckel, W. & Tuschl, T. RNA interference is mediated by 21- and 22-nucleotide RNAs. *Genes Dev.* **15**, 188–200 (2001).
17. Weiss, A. et al. RNAi-mediated silencing of SOD1 profoundly extends survival and functional outcomes in ALS mice. *Mol. Ther.* **33**, 3917–3938 (2025).
18. McCartan, R., Khorkova, O., Volmar, C. H. & Wahlestedt, C. Nucleic acid-based therapeutics for the treatment of central nervous system disorders. *Front. Genet.* **14**, 1250276 (2023).
19. Kang, M. et al. SCAD: a modular platform for efficient delivery of duplex RNA to the CNS and beyond. *Mol. Ther. Nucleic Acids* **36**, 102757 (2025).
20. Duan, C. et al. Intrathecal administration of a novel siRNA modality extends survival and improves motor function in the $SOD1^{G93A}$ ALS mouse model. *Mol. Ther. Nucleic Acids* **35**, 102147 (2024).
21. Hatzipetros, T. et al. A quick phenotypic neurological scoring system for evaluating disease progression in the SOD1-G93A mouse model of ALS. *J. Vis. Exp.* **104**, 53257 (2015).
22. Pfohl, S. R., Halicek, M. T. & Mitchell, C. S. Characterization of the contribution of genetic background and gender to disease progression in the SOD1 G93A mouse model of amyotrophic lateral sclerosis: a meta-analysis. *J. Neuromuscul. Dis.* **2**, 137–150 (2015).
23. Abati, E., Manini, A., Comi, G. P. & Corti, S. Inhibition of myostatin and related signaling pathways for the treatment of muscle atrophy in motor neuron diseases. *Cell. Mol. Life Sci.* **79**, 374 (2022).
24. Ludolph, A. C. et al. Guidelines for the preclinical in vivo evaluation of pharmacological active drugs for ALS/MND: report on the 142nd ENMC international workshop. *Amyotroph. Lateral Scler.* **8**, 217–223 (2007).
25. Chen, W. et al. Clinical and genetic features of patients with amyotrophic lateral sclerosis in southern China. *Eur. J. Neurol.* **27**, 1017–1022 (2020).
26. Lin, J. et al. The distinct manifestation of young-onset amyotrophic lateral sclerosis in China. *Amyotroph. Lateral Scler. Frontotemporal Degener.* **22**, 30–37 (2020).
27. Baird, M. C. et al. Combination AAV therapy with galectin-1 and SOD1 downregulation demonstrates superior therapeutic effect in a severe ALS mouse model. *Mol. Ther. Methods Clin. Dev.* **32**, 101312 (2024).
28. McCampbell, A. et al. Antisense oligonucleotides extend survival and reverse decrement in muscle response in ALS models. *J. Clin. Invest.* **128**, 3558–3567 (2018).

29. Carri, M. T., Grignaschi, G. & Bendotti, C. Targets in ALS: designing multidrug therapies. *Trends Pharmacol. Sci.* **27**, 267–273 (2006).
30. Crow, J. P., Calingasan, N. Y., Chen, J., Hill, J. L. & Beal, M. F. Manganese porphyrin given at symptom onset markedly extends survival of ALS mice. *Ann. Neurol.* **58**, 258–265 (2005).
31. Tortarolo, M. et al. Glutamate AMPA receptors change in motor neurons of SOD1G93A transgenic mice and their inhibition by a noncompetitive antagonist ameliorates the progression of amytrophic lateral sclerosis-like disease. *J. Neurosci. Res.* **83**, 134–146 (2006).
32. Matamala, J. M. & Kiernan, M. C. Natural history and the dawning of a new era for familial ALS. *J. Neurol. Neurosurg. Psychiatry* **88**, 95–96 (2017).
33. Miller, T. et al. Phase 1–2 trial of antisense oligonucleotide tofersen for *SOD1* ALS. *New Engl. J. Med.* **383**, 109–119 (2020).
34. Wiesenfarth, M. et al. Effects of tofersen treatment in patients with *SOD1*-ALS in a 'real-world' setting—a 12-month multicenter cohort study from the German early access program. *eClinicalMedicine* **69**, 102495 (2024).
35. Belgrad, J. et al. The N=1 Collaborative: advancing customized nucleic acid therapies through collaboration and data sharing. *Nucleic Acids Res.* **53**, gkaf346 (2025).

Weiqi Chen (陈玮琪)[1,10], Lingling Jiang (江凌玲)[2,10], Chunling Duan (段春玲)[3,10], Moorim Kang (강무림)[3,10], Jinyi Ye (叶瑾怡)[1], Ling Wang (王玲)[1], Yuesong Pan (潘岳松)[1,2], Hui Qu (曲辉)[1], Xiaoling Liao (廖晓凌)[1], Xuejiao Zhou (周雪姣)[1], Yichen Li (李懿臣)[3], Zubao Gan (甘祖宝)[3], Junnan Chen (陈俊楠)[3], Ian Schacht[3], Robert F. Place[3], Long-Cheng Li (李龙承)[3,4] ✉ & Yilong Wang (王伊龙)[1,2,5,6,7,8,9] ✉

[1]Department of Neurology, Beijing Tiantan Hospital, Capital Medical University, Beijing, China. [2]China National Clinical Research Center for Neurological Diseases, Beijing Tiantan Hospital, Capital Medical University, Beijing, China. [3]Ractigen Therapeutics, Nantong, China. [4]Institute of Reproductive Medicine, Nantong University School of Medicine, Nantong, China. [5]Chinese Institute for Brain Research, Beijing, China. [6]National Center for Neurological Disorders, Beijing, China. [7]Advanced Innovation Center for Human Brain Protection, Capital Medical University, Beijing, China. [8]Beijing Laboratory of Oral Health, Capital Medical University, Beijing, China. [9]Laboratory for Clinical Medicine, Capital Medical University, Beijing, China. [10]These authors contributed equally: Weiqi Chen, Lingling Jiang, Chunling Duan, Moorim Kang. ✉e-mail: lilc@ractigen.com; yilong528@aliyun.com

Methods

Oligonucleotide synthesis and formulation

Oligonucleotides were synthesized in-house using an HJ-12 synthesizer (Highgene-Tech Automation). They were purified through reverse-phase HPLC, quantified by gel electrophoresis and validated using ESI-Centrifugation MS and SEC-HPLC (XBridge Protein BEH SEC 125 Å, Waters). Endotoxin levels were quantified using a Chromogenic Endotoxin Quant Kit (Bioendo). RAG-17 for NHP toxicology studies was synthesized by Wuxi SynTheAll Pharmaceutical (Lot TT-22E029). For in vivo treatments, lyophilized oligonucleotides were dissolved in aCSF immediately before use and diluted to the intended concentrations. Animals were randomly allocated to experimental groups based on body weight, with baseline comparability verified by ordinary one-way analysis of variance (ANOVA; GraphPad Prism). Animals exhibiting poor health before dosing were excluded. The structure of RAG-17 (also named siSOD1-047M3-AC1) can be found in the previous publication[20].

In silico off-target prediction and serum stability assay

In silico off-target prediction. The RAG-17 guide strand was performed using GGGenome (https://gggenome.dbcls.jp) and the miRanda algorithm against the Ensembl human mRNA database[36]. Candidate off-target transcripts were scored based on match/mismatch profiles, including G–U wobble base pairs, and their ranked complementarity to the guide strand. Two categories of candidates were prioritized for experimental validation through RT–qPCR—(1) transcripts harboring three to four mismatches within their 3′ UTRs (*CYTH2*, *NDUFC2*, *DISP2* and *KNOP1*); and (2) *UBAP2L*, which carries one to two mismatches within its coding sequence.

Serum stability assays. Oligonucleotides (3 µM) were incubated at 37 °C with PBS or 50% active human serum for 1–14 days, followed by trypsin treatment (20 µg ml^{-1}, 30 min). Samples were resolved on 20% TBE-Urea polyacrylamide gels at 120 V for 90–120 min and visualized using a ChemiDoc XRS+ System (Bio-Rad).

Cell culture

T98G and COS-1 cell lines (ATCC) were maintained in DMEM with 10% FBS, penicillin–streptomycin and (for T98G cells) 1% nonessential amino acids and 1 mM sodium pyruvate. Cells were maintained at 37 °C with 5% CO_2, and routinely tested for mycoplasma.

In vitro immunotoxicity assay in PBMCs

PBMCs were obtained from healthy non-Chinese donors (OriCell; human immunodeficiency virus/HBV/HCV/syphilis-negative) and fresh blood samples from three healthy volunteers. PBMCs were seeded overnight in 96-well plates at a density of 1×10^6 cells per well. For free uptake experiments, untreated wells served as blanks; 1 µg ml^{-1} lipopolysaccharides and 1 µM CpG ODN2216 (24 h incubation) served as positive controls. Test articles were evaluated in duplicate at 1 µM or 10 µM. For RNAiMAX transfections, cells were transfected with test articles (33 or 133 nM) for 24 h, RNAiMAX alone was used as mock control and 133 nM RAG-IS-1 was used as a positive control. Supernatant cytokine levels were quantified by ELISA (IFN-α—EK182-96, Lot A18220621; human TNF—EK182-96, Lot A18220621; Human IL-1β—70-EK101B-96, Lot A101B20642; Multi Sciences Biotech).

Experimental models and ethics statement

NHP models. Cynomolgus monkeys (3.0–4.0 years old; females 2–3.2 kg, males 2.4–4.4 kg) were obtained from Guangdong Blooming-Spring Biological Technology Development (certifications 44410900000511 and 44410900000512). After quarantine and acclimatization, animals were socially housed at WuXi AppTec (Permit SYXK(Su)2019-0019). The housing conditions included temperatures of 18.6–24.5 °C, 32–82.5% humidity, 10–20 air changes per hour and a 12-h light/12-h dark cycle. All procedures complied with the US Animal Welfare Act, NMPA (CFDA) GLP, US FDA GLP and AAALAC International guidelines, and were approved by the Institutional Animal Care and Use Committee of WuXi AppTec (protocol H59-0027-TX).

Rodent models. Transgenic mice harboring the human *SOD1*^{G93A} mutation (B6.Cg-Tg(*SOD1**G93A)1Gur/J; strain ID 004435) were purchased from the Jackson Laboratory and bred in-house at Nantong University. Mice were group-housed (4–5 per cage) under standard conditions (22 ± 2 °C, 50 ± 10% humidity, 12-h light/12-h dark cycle). Transgenic *SOD1*^{G93A} rats (model 2148) were acquired from Taconic Biosciences and housed in pairs at WuXi AppTec. All rodent procedures complied with NIH and AAALAC guidelines and were approved by the Institutional Animal Care and Use Committees of Nantong University (approval S20220323-001) and WuXi AppTec (approval GP02-QD105-2020V1.0).

In vivo administration and efficacy studies

ICV injections in mice. Under freshly prepared 1.2% avertin anesthesia (0.30–0.35 ml/10 g), a 25-gauge needle was stereotaxically placed at 0.2 mm anterior–posterior and 1.0 mm mediolateral (right) from bregma. A total of 10 µl of either aCSF vehicle or RAG-17 was injected into the lateral ventricle at approximately 1 µl s^{-1}. For the early-treatment regimen, *SOD1*^{G93A} mice received two ICV injections of aCSF or 400 µg RAG-17 on PNDs 70 and 100. For the late-treatment regimen, two ICV injections of 200 or 400 µg RAG-17 were administered on PNDs 126 and 151.

Intrathecal injections in rats. Under 3.0% isoflurane anesthesia, a 30-gauge needle was inserted into the L5–L6 interspace until a tail flick reflex was observed. A 30-µl bolus was injected slowly over 1 min. Female *SOD1*^{G93A} rats received two intrathecal injections of either NTC or 900 µg RAG-17 on day 0 (PND 70) and day 60 (PND 130). WT littermates received aCSF as a vehicle control. Blinding was applied to the treatment groups.

PK and tissue distribution (liquid chromatography tandem–mass spectrometry)

Rat tissue distribution study. Sprague–Dawley rats (n = 24, 12 animals per sex) received a single intrathecal dose of RAG-17 (1.0 mg/30 µl). Rats were killed at days 1, 7, 28 and 42 (n = 6 per time point, three animals per sex). Brain regions (for example, brain stem, cerebellum, frontal cortex, hippocampus, striatum, cerebrum), spinal cord segments (for example, lumbar, cervical, thoracic) and peripheral tissues (for example, spleen, liver, kidney, lung, heart and muscle) were collected and homogenized on ice (1:9 wt/vol) in lysis buffer (Phenomenex).

Monkey PK study. Forty cynomolgus monkeys (20 animals per sex, ~3 to 4 years of age) were randomized into four groups (five animals per sex per group) receiving either vehicle (aCSF) or RAG-17 at 5, 20 or 50 mg dose^{-1}. Two intrathecal doses were administered on days 1 and 15 via the L4–L5 intervertebral space. CSF (1:1 with stabilizing buffer) was collected at 15 min, day 22 and day 71. Subgroups were killed on day 22 (dosing group; n = 6 per group, equally by sex) and day 71 (recovery group; n = 4 per group, equally by sex). Brain (for example, cerebral cortex) and spinal cord (for example, cervical, thoracic, lumbar) tissues were collected.

Quantification. RAG-17 concentrations were determined using validated methods at WuXi AppTec. The specific assay methods were H59-0049-VM for brain tissue and H59-0050-VM for spinal cord tissue. Data were collected by Analyst and processed using Watson LIMS. The linear dynamic range was 50.0–25,000 ng g^{-1} (rat tissues) and 20.0–8,000 ng ml^{-1} (monkey CSF and plasma).

Gene expression analysis (RT–qPCR)

Total RNA was extracted from RNAlater-preserved frozen tissues or cultured cells using either Total RNA Isolation Reagent (Biosharp) or RNAzol (Vigorous). RNA samples were then purified using the RNeasy RNA kit (Qiagen). RT was performed using the PrimeScript RT kit (Takara). The resulting cDNA was amplified in triplicate on a LightCycler 480 real-time PCR system (Roche) using SYBR Premix Ex Taq II (Takara). Amplification was conducted with target-specific primers alongside species-specific internal controls (*TBP* for human; *GAPDH* for cynomolgus monkey; primer sequences are provided in Supplementary Information). Primer specificity was verified through melting curve analysis. Relative gene expression was calculated using the ΔΔCt method, and knockdown percentage (%) was determined as (1 − (relative target gene level)) × 100.

Histology, RNAscope and SOD1 ELISA

Histology and immunohistochemistry. L4–L5 rat spinal cord segments were fixed in cold 4% paraformaldehyde, paraffin-embedded and sectioned (4-µm thickness). After antigen retrieval in citrate buffer (pH 6.0, 90 °C), sections were labeled with an anti-ChAT antibody (AB144P, Merck Millipore; 1:400) overnight at 4 °C, followed by incubation with an HRP-conjugated antigoat IgG secondary antibody.

ISH (RNAscope). After intrathecal administration of RAG-17 (1.6 or 4.8 mg) or saline in Sprague–Dawley rats, brain and spinal cord tissues were collected and paraffin embedded. The biodistribution of the oligonucleotide was analyzed on the tissue sections using the miRNAscope HD Reagent Kit–RED (ACDbio) with a custom-designed antisense probe (ACDbio-1199511-S1) following the manufacturer's instructions.

Quantification of SOD1 protein. Monkey CSF SOD1 levels were quantified by sandwich ELISA (AE17754MK, Abebio). Samples were incubated in microtiter plates precoated with a capture antibody, followed by sequential incubations with a biotin-conjugated detection antibody and streptavidin-HRP. Optical density was measured at 450 nm (with a correction at 540 nm).

Study design and participants in clinical trial of RAG-17

We performed an open-label, single-center and dose-escalation clinical trial to investigate the safety and tolerability of RAG-17 in patients with ALS with *SOD1* gene mutation (CREATION). This clinical trial was approved by the Ethics Committee of Beijing Tiantan Hospital (ethical approval KY2023-015-02) and obtained record-filing approval from the Human Genetic Resources Administration of China. The study was registered with NCT05903690 on 24 May 2023. Written informed consent was obtained from the participants or their legal representatives before enrollment. Six eligible patients from China were enrolled between May 2023 and July 2024. The study was conducted in accordance with the CONSORT framework for transparent reporting of clinical trials.

Patients with *SOD1*-associated ALS were enrolled based on the following inclusion criteria: (1) deemed medically suitable to complete the trial; (2) aged between 18 and 75 years, irrespective of sex; (3) a confirmed diagnosis of ALS with a documented known *SOD1* mutation associated with reported disease progression; (4) FVC of ≥50% predicted value during the screening period; (5) diagnosis of patients meeting the revised El Escorial criteria for confirmed or probable familial or sporadic ALS, as established by the World Federation of Neurology[37]; (6) provision of written informed consent by the patient or their legal representative and (7) commitment to use effective contraception, with no plans for reproduction or gamete donation during the study and for 3 months thereafter. The exclusion criteria were as follows: (1) carriers of specific *SOD1* mutations (nucleotide positions 44–66 from the start of SOD1 protein translation or p.F21C); (2) patients who had previously received or were currently receiving tofersen treatment; (3) a positive test result for human immunodeficiency virus, current or historical; (4) a positive test result for hepatitis C virus antibody, current or historical; (5) active hepatitis B infection (hepatitis B surface antigen positive and/or hepatitis B core antibody positive); (6) the use of other investigational drugs within 30 days or 5 half-lives before screening; (7) contraindications to lumbar puncture; (8) patients with other known diseases related to MN dysfunction that could confound the diagnosis of ALS; (9) a psychiatric disorder diagnosed per Diagnostic and Statistical Manual of Mental Disorders, Fifth Edition (DSM-5) criteria or exhibiting active suicidal ideation; (10) combined with severe liver dysfunction (ALT value or aspartate aminotransferase (AST) value of ≥2.0× the upper limit of normal value), renal dysfunction (serum creatinine of ≥1.5× the upper limit of normal value or estimated glomerular filtration rate of <40 ml min^{-1} 1.73 m^{-2}) or severe heart dysfunction (New York Heart Association Class III or IV); (11) permanent mechanical ventilation dependence; (12) history of alcohol or substance abuse; (13) pregnancy, lactation or intent to conceive; (14) concurrent enrollment in another clinical trial involving an investigational therapy; (15) recent vaccination (within 28 days); (16) contraindications for magnetic resonance imaging (MRI; that is, claustrophobia) and (17) any other condition that may interfere with follow-up.

Clinical procedures and dosing regimen

RAG-17 was provided as a dry powder by Ractigen Therapeutics. Before administration, it was reconstituted to 5 ml with aCSF. Patients received a single injection between the L2 and L5 lumbar vertebrae based on the investigator's judgment per visit, on days 1, 15, 29, 60, 120, 180 and 240, for a total of six or seven injections. The first three participants initiated treatment at 60 mg, while the subsequent three began at 90 mg. During the dose-escalation phase (dosing every 2 weeks), the dose was increased by 30 mg per subsequent treatment. During the dose-maintenance phase, a fixed dose was administered every 2 months over an 8-month cycle (Fig. 4a).

Clinical outcomes

The primary endpoints included the following safety evaluation measures: (1) incidence of adverse events (AEs) and SAEs within 240 days after RAG-17 treatment; (2) changes in laboratory assessments, vital signs, ALSFRS-R scores and incidence of abnormalities in heart, lung and abdomen examinations, neurological examinations, as well as ECG within 240 days after the first injection of RAG-17. The ALSFRS-R consists of 12 items across four subdomains of bodily function (bulbar, fine motor, gross motor and breathing). Each item is scored on an ordinal scale from 0 (total loss of function) to 4 (no loss of function), yielding total scores ranging from 0 to 48, with higher scores indicating better function[38].

The secondary endpoints included (1) changes in CSF SOD1 protein levels at days 15, 29, 60, 120, 180 and 240 from baseline; (2) changes in plasma NfL levels at days 1, 15, 29, 60, 120, 180 and 240 from baseline; (3) PK of RAG-17 in plasma at days 1, 15, 29, 60, 120, 180 and 240; and (4) time to invasive mechanical ventilation or death.

The exploratory endpoints included changes in (1–7) pulmonary function (including FVC), fatigue severity, muscle strength, gait function, modified Norris scale scores, quality of life and clinical staging, at assessed at days 15, 29, 90, 180 and 240; and (8–9) electromyography and 7 T MRI imaging features, assessed at days 29, 90, 180 and 240. Fatigue severity was assessed using the FSS[39]. Evaluation of gait function included three-dimensional gait analysis, short physical performance battery, tandem walking and the 6-m walk test. Quality of life was estimated using the ALSAQ-40, a five-level version of the EQ-5D-5L, the HAMA and the HAMD. Clinical staging was evaluated using the London ALS Stage[40] and Milano–Torino staging[41]. The electromyographic features evaluated in this study included the composite muscle action potentials, motor unit number index and motor unit size index.

All clinical outcomes were adjudicated by the clinical event adjudication committee, which was composed of independent experts with extensive clinical experience.

Laboratory assessments

Laboratory assessments, including complete blood count, basic metabolic panel and CSF biochemistry, were performed at the central laboratory of Beijing Tiantan Hospital. CSF SOD1 (ELISA; BMS222TEN, Thermo Fisher Scientific) and plasma NfL (Ella, ProteinSimple) were quantified in duplicate and triplicate, respectively, at a certified third-party laboratory (United-Power Pharma Tech). CSF NfL was measured retrospectively at Beijing Tiantan Hospital by chemiluminescence immunoassay (Human Neurofilament Light Chain (NfL) Assay Kit, Vazyme).

Protocol amendments

The study protocol underwent four approved amendments. From v1.1 to v1.2 (February–April 2023), to minimize patient burden from lumbar punctures, CSF SOD1 measurement at day 1 (secondary endpoint) was removed, and PK analysis was limited to plasma. From v1.2 to v1.3 (April–June 2023), the PK blood sampling schedule was optimized with more frequent early time points (1, 2, 4, 6, 12 and 48 h instead of 15 min, 4 h, 48 h and 4 days postdose). From v1.3 to v2.0 (June–August 2023), FVC inclusion threshold was lowered from ≥80% to ≥50% of predicted to facilitate enrollment by broadening the eligible population. The dosing regimen was specified–fourth dose of 120 mg, fifth dose of 150–180 mg (maximum 180 mg). From v2.0 to v2.1 (August–October 2023), the primary safety and tolerability evaluation period was extended from 180 to 240 days (aligned with the final dose), with all exploratory endpoint assessments prolonged accordingly. The fourth dose increased from 120 mg to 150 mg. The drug storage condition was revised from −20 ± 5 °C to 2–8 °C. All amendments were approved by the institutional ethics committee before enrolling relevant patients.

Ethical considerations and participant enrollment in clinical trial of RAG-17

This clinical trial was approved by the Ethics Committee of Beijing Tiantan Hospital (KY2023-015-02). Six eligible patients were enrolled from 22 May 2023 to 27 November 2023 in China. Written informed consent was obtained from all participants or their legally authorized representatives before enrollment in accordance with the Declaration of Helsinki. Participants received a fixed travel allowance and a modest reimbursement for blood and CSF collection procedures; no other compensation was provided for study participation. This report incorporates data from all participants who received RAG-17 during the study. The data collection period spanned from 24 May 2023 to 11 July 2024. The final dataset was locked as of 8 October 2024.

Sex and gender considerations

Sex or gender information was collected based on self-reporting. No sex-based or gender-based subgroup analysis was performed because the study objectives were designed independently of sex or gender.

Statistics and reproducibility

Analysis of preclinical data. All statistical analyses were performed using GraphPad Prism software (v11.0.0; 84). Quantitative data are presented as mean ± s.d. or mean ± s.e.m., as indicated in the respective figure legends. For comparisons between two groups, Welch's *t* test was used. In specific instances, evaluating a specified direction of change, a one-tailed test was applied. For comparisons among three or more groups, statistical significance was determined by one-way ANOVA followed by Dunnett's or Tukey's multiple comparisons test. For data involving multiple groups and time points, a two-way ANOVA followed by Bonferroni's multiple comparison test was used. Survival and disease-onset data were analyzed using the Kaplan–Meier method, and statistical significance was determined using the log-rank (Mantel–Cox) test. A P value <0.05 was considered statistically significant (*P < 0.05; **P < 0.01; ***P < 0.001; ****P < 0.0001).

Reproducibility. For in vitro assays (for example, serum stability, RT–PCR and cytokine measurements), experiments were performed with biologically independent samples (n = 2 or 3 per group per donor) and were successfully replicated independently at least twice. For in vivo studies, the reported n values represent biologically independent animals, with group sizes ranging from 3 to 20 depending on the experimental endpoint. All histological evaluations, including ISH and ChAT staining, were performed on multiple sections per animal (for example, averaged across two separate sections per animal in the L4–L5 region), and assessments were conducted in a blinded manner to the experimental conditions. Representative images were selected from independent biological replicates (n = 3–20 per group), and the results showed consistent outcomes across replicates.

Study design and sample size. No statistical method was used to predetermine sample size. Sample sizes (for example, n = 10–20 for rodent efficacy models, n = 4–6 for NHPs and n = 3 for in vitro and PK analyses) were chosen based on standard practices in the field to ensure adequate statistical power for evaluating the therapeutic efficacy and PD of RAG-17.

Data exclusion. For the exposure–response correlation analyses in cynomolgus monkeys, samples with tissue concentrations below the limit of quantification were excluded (resulting in n = 23 for spinal cord and n = 11 for brain analyses). Otherwise, no data were excluded from the analyses.

Randomization and blinding. Animals were randomly assigned to treatment groups. Behavioral assessments were performed by investigators blinded to the treatment allocations.

Analysis of clinical data

Given the small sample size and exploratory nature of this study, the analysis was descriptive, and no formal inferential hypothesis testing was performed. Data are presented for all six enrolled participants. No statistical method was used to predetermine the sample size and the investigators were not blinded to allocation during experiments and outcome assessment. No data were excluded from the analyses, and the study was not randomized.

Categorical or ordinal variables (including AEs and SAEs) were described by frequency and percentage, stratified by trial visit and dose cohort. Continuous variables, including biomarker levels (for example, SOD1 and NfL) and clinical scores (for example, ALSFRS-R), are summarized using descriptive statistics (for example, measured concentrations or mean with s.d.) or presented graphically. Specifically, for SOD1 and NfL protein, two types of figures were generated—individual sample concentrations across visits and mean percentage (±s.e.) change from baseline by cohort. Longitudinal changes in clinical scores, including ALSFRS-R, FVC, FSS, gait function, modified Norris scale scores, ALSAQ-40, EQ-5D-5L, HAMA, HAMD and clinical staging during the follow-up period, were described using line charts. Selected laboratory tests, muscle strength, electromyography parameters, specific gait function metrics and the London ALS stage were presented directly as measured values in Supplementary Tables 1–65 and 67–102.

For PK data, individual and mean (±s.e.) concentration–time profiles were plotted by dose cohort. No adjustments were made, and no covariates were formally tested in models due to the descriptive design. Exploratory post hoc analyses were performed, including changes in body weight, CSF protein and NfL, as well as changes in ALSFRS based on baseline disease severity and duration. Statistical analyses were performed with SAS software (v9.4; SAS Institute).

Reporting summary
Further information on research design is available in the Nature Portfolio Reporting Summary linked to this article.

Data availability
All primary data supporting the findings of this study are included in this article and its Supplementary Information. Individual de-identified participant data that support the findings of this study are not publicly available due to privacy and ethical restrictions. These data are stored on the secure server of the China National Clinical Research Center for Neurological Diseases and can be accessed under controlled conditions to verify the research conclusions. Access to these data is granted to qualified researchers following a review and approval process managed by the Center's data access committee. Researchers who provide a methodologically sound analysis proposal that complies with clinical study ethical and data integrity requirements can request access through the Center's Data Management and Sharing System (https://paper.ncrcnd.org.cn) or by contacting the corresponding author (Y.W.). Requests will be evaluated within 30 days. The study protocol and statistical analysis plan are available in Supplementary Data (Protocol and SAP), respectively. Source data are provided with this paper.

References

36. Enright, A. J. et al. MicroRNA targets in *Drosophila*. *Genome Biol.* **5**, R1 (2003).
37. Brooks, B. R., Miller, R. G., Swash, M. & Munsat, T. L. El Escorial revisited: revised criteria for the diagnosis of amyotrophic lateral sclerosis. *Amyotroph. Lateral Scler. Other Motor Neuron Disord.* **1**, 293–299 (2009).
38. Cedarbaum, J. M. et al. The ALSFRS-R: a revised ALS functional rating scale that incorporates assessments of respiratory function. BDNF ALS Study Group (phase III). *J. Neurol. Sci.* **169**, 13–21 (1999).
39. Krupp, L. B., LaRocca, N. G., Muir-Nash, J. & Steinberg, A. D. The fatigue severity scale. Application to patients with multiple sclerosis and systemic lupus erythematosus. *Arch. Neurol.* **46**, 1121–1123 (1989).
40. Roche, J. C. et al. A proposed staging system for amyotrophic lateral sclerosis. *Brain* **135**, 847–852 (2012).
41. Balendra, R. et al. Use of clinical staging in amyotrophic lateral sclerosis for phase 3 clinical trials. *J. Neurol. Neurosurg. Psychiatry* **86**, 45–49 (2015).

Acknowledgements
The authors would especially like to thank all patients and team members for their contributions.

Author contributions
L.-C.L., W.C. and Y.W. designed the study. L.-C.L., L.J., J.Y., C.D., M.K., W.C. and Y.W. interpreted the data. C.D. and M.K. conceived of and supervised the preclinical studies. C.D., Z.G. and J.C. conducted the preclinical studies. L.J., J.Y., L.W., H.Q., X.L., X.Z. and W.C. performed the patient enrollment, diagnosis and clinical follow-up. Y.P. contributed to the acquisition and analysis of data. L.J., J.Y., C.D. and M.K. wrote the paper, which was further revised by Y.L., I.S., R.F.P., L.-C.L., W.C. and Y.W. All authors have read and approved the paper.

Funding
This work was supported by the National Natural Science Foundation of China (grant 82425101 to Y.W.), Beijing Scholar Program (grant 120 to Y.W.), Beijing Nova Program (grant 20230484245 to W.C.), Noncommunicable Chronic Diseases—National Science and Technology Major Project (grants 2023ZD0504800, 2023ZD0504801, 2023ZD0504802, 2023ZD0504803 and 2023ZD0504804 to Y.W.), Capital's Funds for Health Improvement and Research (grant 2022-2-2045 to Y.W.), National Key R&D Program of China (grants 2022YFF1501500, 2022YFF1501501, 2022YFF1501502, 2022YFF1501503, 2022YFF1501504 and 2022YFF1501505 to Y.W.), Beijing Laboratory of Oral Health (grant PXM2021_014226_000041 to Y.W.), Beijing Municipal Science & Technology Commission (grant Z231100004823036 to Y.W.) and Ractigen Therapeutics (grant HX-A-2023004 to Y.W.). The funders had no role in the study design, data collection, analysis, interpretation or the writing of this manuscript.

Competing interests
L.-C.L., C.D., M.K., Y.L., Z.G., J.C., I.S. and R.F.P. were employed by Ractigen Therapeutics during the completion of this work. L.-C.L. and M.K. hold shares in Ractigen Therapeutics and are inventors on patents RAG-17 assigned to the company (as described in this study). The other authors declare no competing interests.

Additional information
Extended data is available for this paper at https://doi.org/10.1038/s41591-026-04491-7.

Supplementary information The online version contains supplementary material available at https://doi.org/10.1038/s41591-026-04491-7.

Correspondence and requests for materials should be addressed to Long-Cheng Li or Yilong Wang.

Peer review information *Nature Medicine* thanks Aaron Gitler and the other, anonymous, reviewer(s) for their contribution to the peer review of this work. Primary Handling Editor: Anna Ranzoni, in collaboration with the *Nature Medicine* team.

https://doi.org/10.1038/s41591-026-04491-7

Extended Data Table 1 | Tissue pharmacokinetic parameters of RAG-17

Tissue	Parameters in male rats (n = 3)				Parameters in female rats (n = 3)			
	Cmax	Tmax	AUC0-last	T1/2	Cmax	Tmax	AUC0-last	T1/2
	(ng/g)	(h)	(ngh/g)	(days)	(ng/g)	(h)	(ngh/g)	(days)
Liver	18,200	6	3640,000	6.2	29,900	6	4,140,000	8.1
Kidney	55,800	6	11,300,000	6.6	75,600	6	33,100,000	9.2
Lung	677	6	172,000	21.9	636	144	234,000	NR
Heart	521	6	191,000	25	722	6	222,000	8.6
Muscle	ND	ND[a]	ND	ND	ND	ND	ND	ND
Spleen	7,910	6	3,370,000	13	11,100	6	2,910,000	11.5
Brain[b]	3,230	144	2,340,000	NR[c]	2,900	6	1,310,000	NR
Brain stem	3,510	144	2,160,000	NR	2,950	6	1,040,000	NR
Cerebellum	7,410	6	4,470,000	NR	8,370	6	2,160,000	NR
Cervical spinal	7,770	6	4,020,000	27.3	6,040	6	1,850,000	NR
Frontal cortex	1,670	144	1,400,000	NR	1,790	6	858,000	NR
Hippocampus	2,410	144	14,00,000	NR	3,180	6	802,000	NR
Lumber spinal	65,900	6	22,600,000	21	75,000	6	13,500,000	NR
Striatum	304	144	197,000	20.1	ND	ND	ND	ND
Thoracic spinal	26,100	6	11,800,000	23.1	26,500	6	6,480,000	NR

[a]ND, not determined as more than half (>50%) of the individual values are not quantifiable. [b]Brain, the remaining brain tissues. [c]NR, not reportable.

https://doi.org/10.1038/s41591-026-04491-7

Extended Data Table 2 | Longitudinal body weight (kg) changes of the six subjects during the trial

Patients	Baseline	Day 15	Day 29	Day 60	Day 90	Day 120	Day 180	Day 240
Case 1	115	113	115	112	113	111	113	115
Case 2	44	44	44	44	43	43	43	43
Case 3	40	45	45	43	46	–	–	–
Case 4	60	60	60	–	60	60	–	–
Case 5	60	60	60	–	–	60	59	58
Case 6	59	59	60	–	–	60	60	60

https://doi.org/10.1038/s41591-026-04491-7

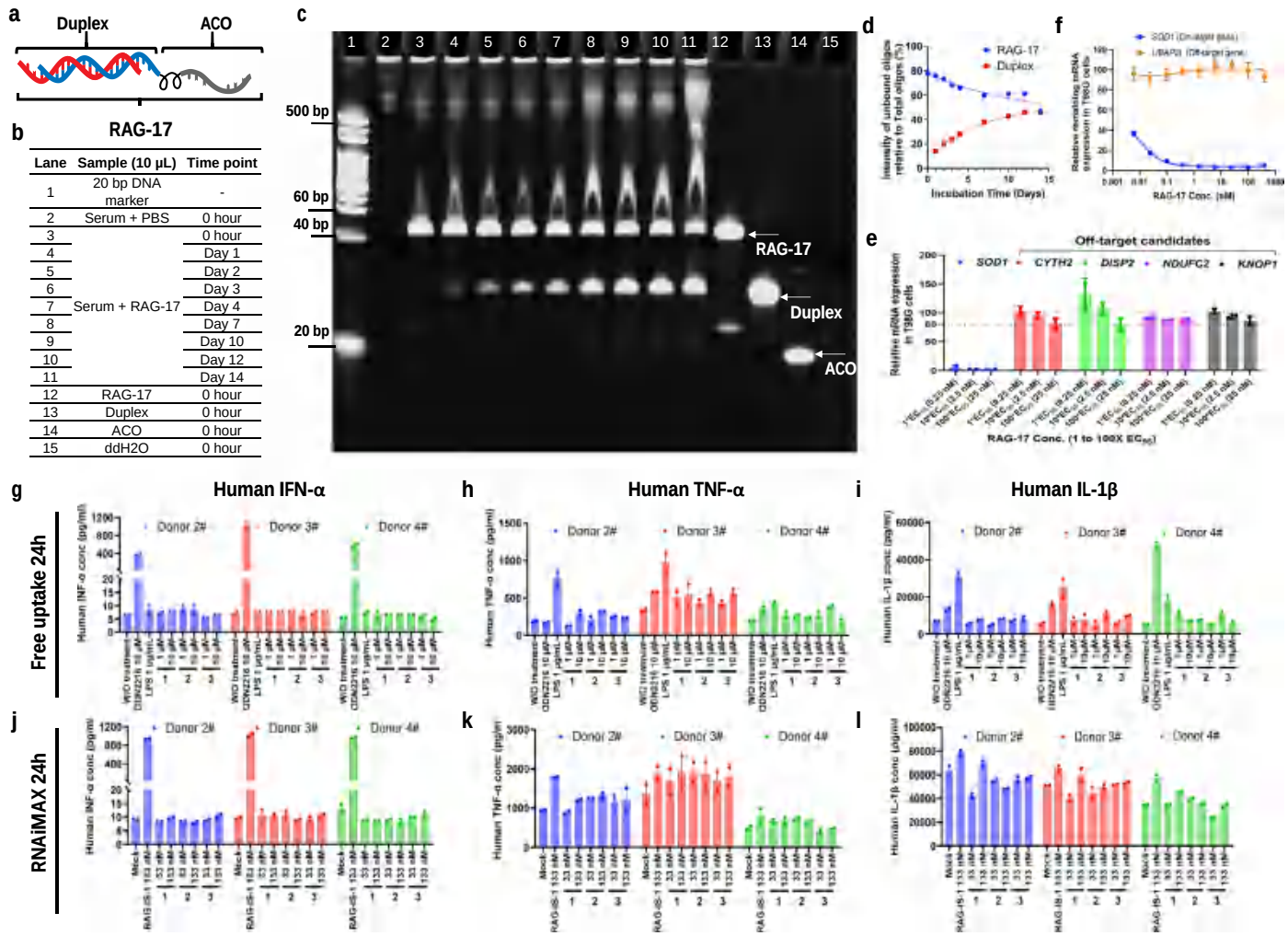

Lane	Sample (10 µL)	Time point
1	20 bp DNA marker	-
2	Serum + PBS	0 hour
3	Serum + RAG-17	0 hour
4		Day 1
5		Day 2
6		Day 3
7		Day 4
8		Day 7
9		Day 10
10		Day 12
11		Day 14
12	RAG-17	0 hour
13	Duplex	0 hour
14	ACO	0 hour
15	ddH2O	0 hour

Extended Data Fig. 1 | In vitro characterization of RAG-17. a, Schematic of the SCAD architecture comprising a duplex conjugated to an ACO via a linker. **b**, Lane loading information for the serum stability assay shown in **c**. **c**, Serum stability assay. Oligonucleotides (RAG-17, its duplex component, and its ACO component) at 3 µM were incubated with an equal volume of active human serum (final concentration of 50% vol/vol) at 37 °C for indicated durations (days 0, 1, 2, 3, 4, 7, 10, 12, and 14) and separated by 15% denaturing polyacrylamide gel electrophoresis (PAGE). Control samples mixed with PBS instead of serum served as the 100% intact oligonucleotide control (lane 12–14). **d**, Relative band intensity quantification of the intact RAG-17 and its free duplex component from the gel panel **c**. **e**,**f**, Off-target analysis in T98G cells. **e**, RT-PCR analysis following transfection with RAG-17. RAG-17 was tested at concentrations of 0.25, 2.5, and 25 nM, representing up to 100-fold its IC95 for on-target activity, relative to mock treatment. Expression levels of selected genes (*CYTH2*, *NDUFC2*, *DISP2*, and *KNOP1*) with predicted off-target sites in their 3′ UTRs containing 3–4 mismatches to RAG-17 were analyzed. Off-target candidates were predicted using miRanda to mine Ensembl sequence cataloged within the biomaRT database comprising the entire human transcriptome. **f**, Complete dose-response curve for *UBAP2L* expression, which carries 1–2 mismatches in flank region of RAG-17 and target its CDS. **g**–**i**, Innate immune response (gymnotic delivery). Oligonucleotides (RAG-17, its duplex, or its ACO component) at 1 µM or 10 µM were added to isolated PBMCs from 3 healthy donors. After 24 h, IFN-α (**g**), TNF (**h**), and IL-1β (**i**) levels in the supernatants were measured by ELISA. Mock: cells treated with vehicle/media only (without oligonucleotides). ODN2216: CpG ODN2216 (a known TLR9 agonist); LPS: lipopolysaccharide (positive controls); W/O: untreated blank control. Data are presented as mean ± s.d. of n = 2 biological replicates for each individual donor. Individual dots represent the biological replicates. **j**–**l**, Innate immune response (transfection). Oligonucleotides (RAG-17, its duplex, or its ACO component) were transfected using RNAiMAX into isolated PBMC from 3 healthy donors at 33 nM or 133 nM. After 24 h, IFN-α (**j**), TNF (**k**), and IL-1β (**l**) levels in the supernatants were measured by ELISA. Mock: cells transfected with RNAiMAX only (without oligonucleotides). Data are presented as mean ± s.d. of n = 2 biological replicates for each individual donor. Individual dots represent the biological replicates.

https://doi.org/10.1038/s41591-026-04491-7

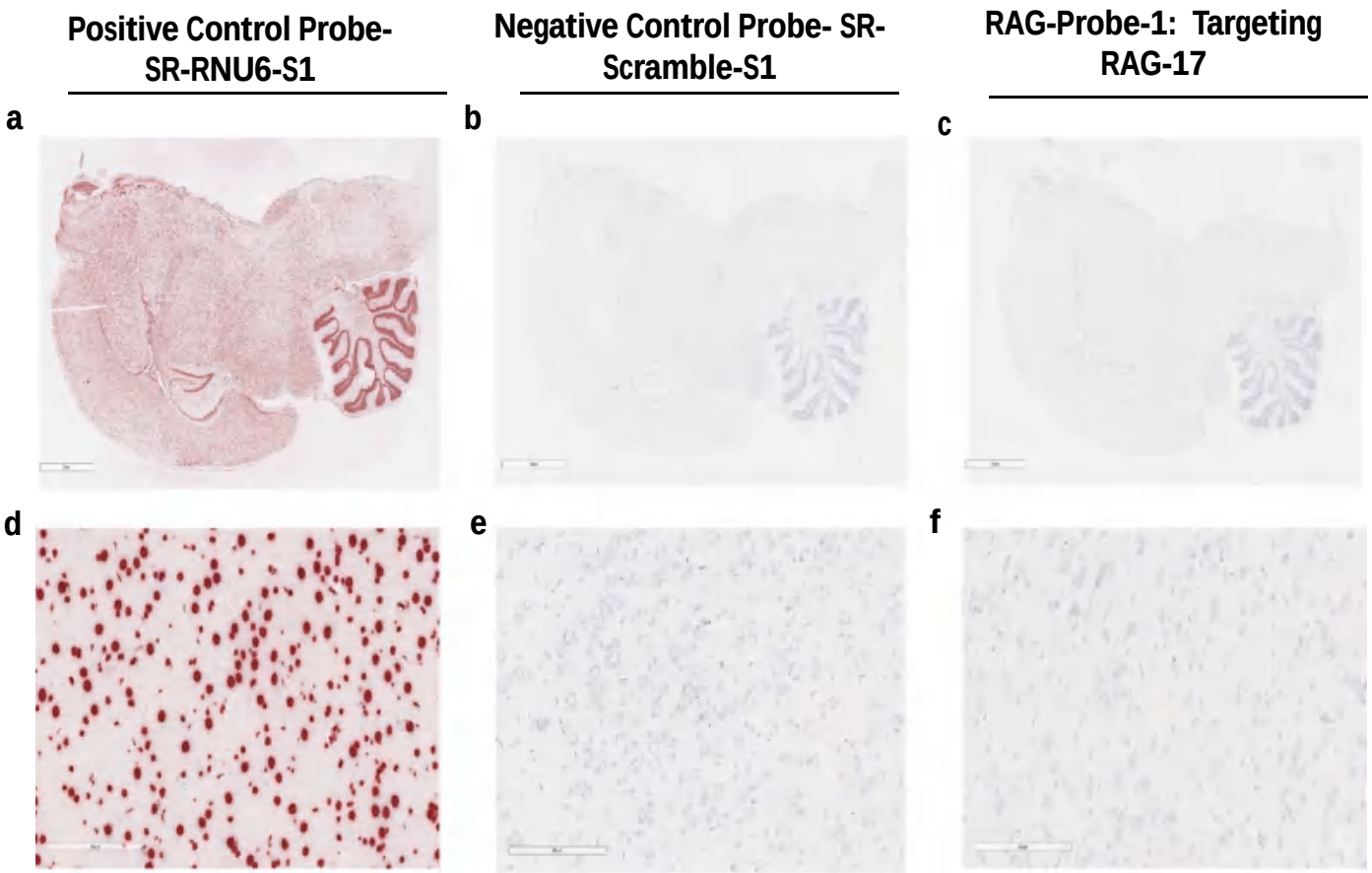

Extended Data Fig. 2 | Specificity of RNAscope assay. a–**c**, Assay validation of RNAscope probes. A positive control (SR-RNU6-S1, designed to hybridize with the ubiquitously expressed U6 small nuclear RNA) (**a**) and a negative control probe (SR-Scramble-S1, a scrambled sequence lacking homology to any known mammalian RNA) (**b**) were used to validate assay specificity and quality. These validation experiments were performed on paraffin-embedded brain sections from vehicle (aCSF)-treated control rats (**c**). **d**–**f**, Enlarged images corresponding to panels **a**–**c**, respectively. RNA signal is shown in red; nuclei were counterstained with hematoxylin. Scale bars: Panels **a**–**c**: 6 mm (representing whole brain sections). Panels **d**–**f**: 200 µm (representing magnified regions).

https://doi.org/10.1038/s41591-026-04491-7

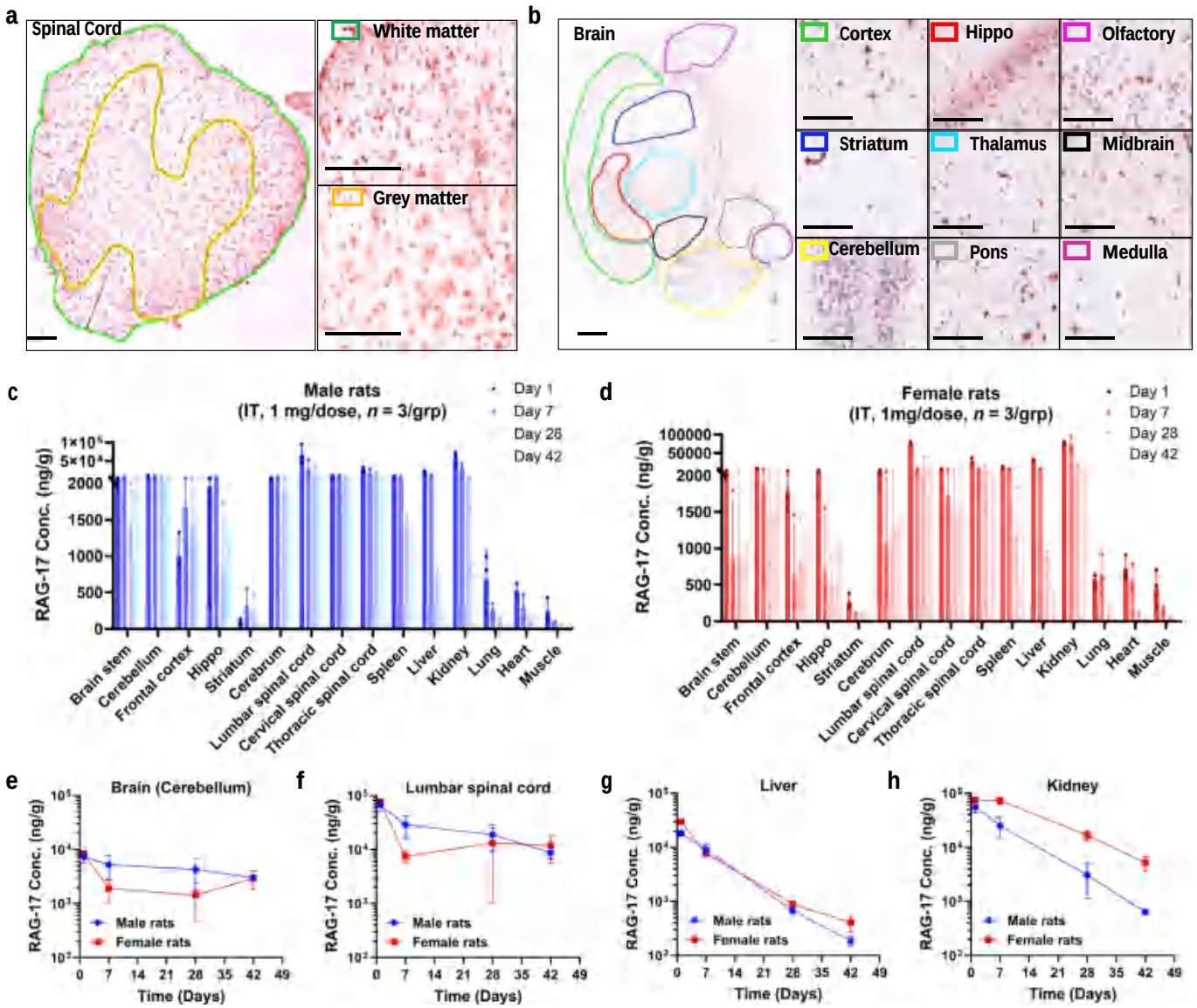

Extended Data Fig. 3 | Tissue distribution and PK profile of RAG-17 after single intrathecal administration in rats. a,**b**, In situ hybridization (ISH) analysis. Sprague-Dawley (SD) rats were administered with a single intrathecal (IT) dose of RAG-17 (4.8 mg) and killed on day 15. Tissues were formalin-fixed and paraffin-embedded. Representative images show RAG-17 distribution in the lumbar spinal cord (**a**) and various brain regions (cortex, hippocampus, olfactory bulb, striatum, thalamus, midbrain, cerebellum, pons and medulla) (**b**). The RNA signal is shown as red; nuclei were counterstained with hematoxylin. Scale bars: 6 mm (whole brain/spinal cord) and 200 µm (magnified regions). **c**,**d**, PK. Rats received a single IT dose of RAG-17 (1.0 mg) and were killed at designated time points for tissue collection and siRNA quantification via LC–MS/MS. siRNA concentrations in different tissues over time are shown for male (**c**) and female (**d**) rats. Data are presented as mean ± s.d. with individual data points overlaid ($n = 3$ biologically independent animals per time point for each sex). **e**–**h**, PK profiles over time in the brain (cerebellum, **e**), spinal cord (lumbar, **f**), and peripheral tissues (liver, **g**; kidney, **h**). Data represent mean ± s.e.m. of biologically independent animals ($n = 3$) per time point for each sex.

https://doi.org/10.1038/s41591-026-04491-7

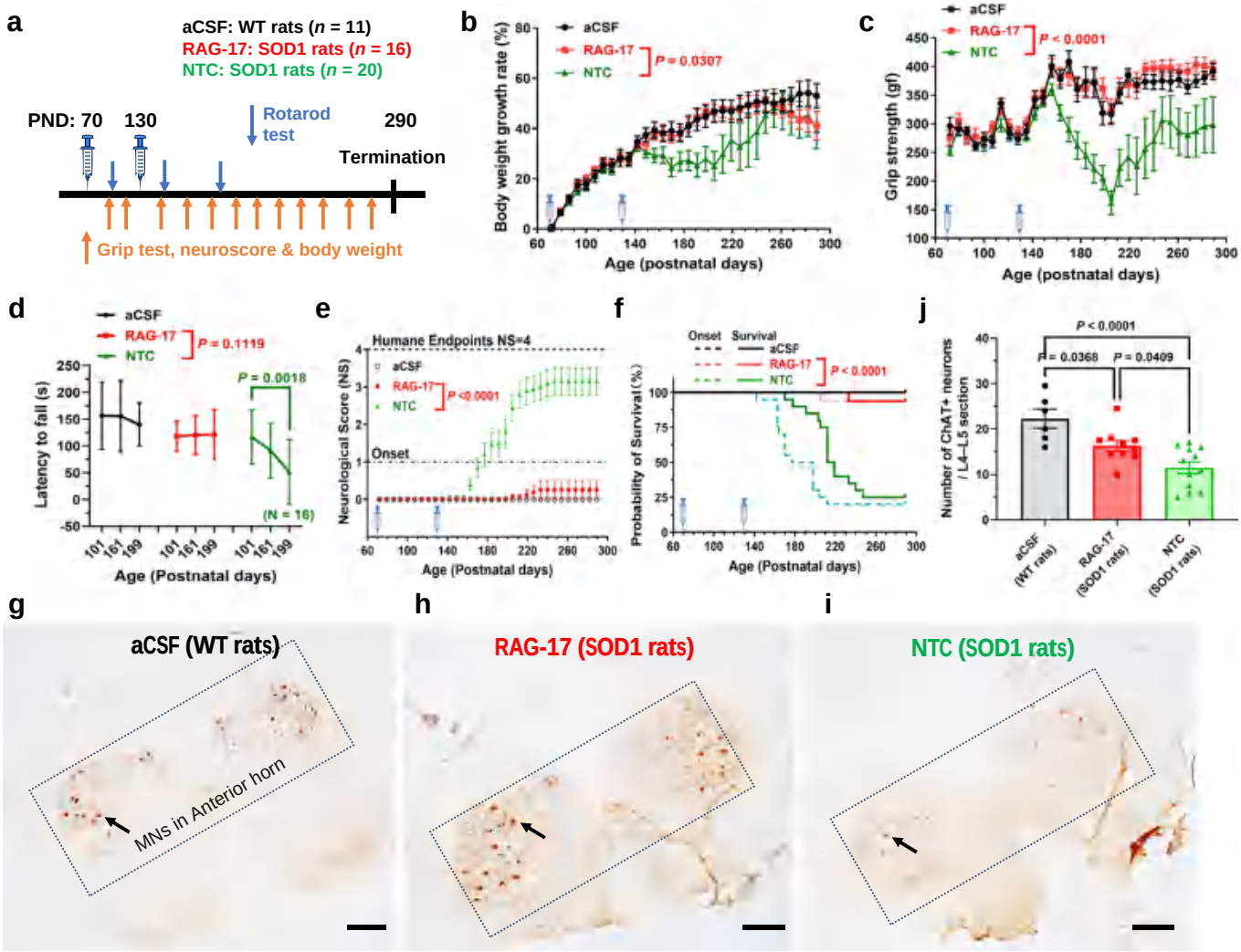

Extended Data Fig. 4 | Therapeutic efficacy of RAG-17 in *SOD1*^{G93A} rats. Female *SOD1*^{G93A} rats (NTac:SD-Tg(*SOD1*^{G93A})L26H) and wild-type (WT) littermates (NTac:SD) were used. *SOD1*^{G93A} rats received a nontargeting control (NTC) or RAG-17 (0.9 mg per dose) via intrathecal (IT) injection on PND 70 and PND 130. **a**, Schematic of the study design showing two IT doses in WT and *SOD1*^{G93A} rats. **b**, Body weight change (%) relative to baseline. **c**, Muscle grip strength. For panels **b** and **c**, data are presented as mean ± s.e.m. of biologically independent animals (WT-aCSF: $n = 11$; *SOD1*^{G93A}-NTC: $n = 20$; *SOD1*^{G93A}-RAG-17: $n = 16$). Statistical analysis was performed using a two-way ANOVA followed by Bonferroni's multiple comparison test. **d**, Motor function assessed by the rotarod test (latency to fall at 4 rpm within a 5-min cutoff) on PND 101, 161, and 199. Data are presented as mean ± s.d. of biologically independent animals. **e**, Neurological score analysis determining median disease onset (defined as a neurological score = 1) and lifespan (defined as a neurological score = 4, humane endpoint). **f**, Kaplan–Meier survival curves. For panels **e** and **f**, statistical significance was determined by the log-rank (Mantel–Cox) test. **g**–**i**, Representative images of ChAT-stained motor neurons (MNs) in the ventral horn of L4–L5 lumbar spinal cord cross-sections. Shown are (**g**) a WT vehicle (aCSF)-treated rat, (**h**) a RAG-17-treated *SOD1*^{G93A} rat, and (**i**) an NTC-treated *SOD1*^{G93A} rat. Arrows indicate ChAT-positive MNs. Scale bar: 100 µm. **j**, Quantification of ChAT-positive neurons averaged from two separate sections per animal in the L4–L5 region. Data are presented as mean ± s.d. (aCSF: $n = 6$; RAG-17: $n = 10$; NTC: $n = 12$). Statistical analysis was determined by Welch's *t*-test for **b, c**, and **e** (comparing RAG-17 vs. NTC), and by one-way ANOVA followed by Tukey's multiple comparison test for **d** and **j**. A one-tailed test was used where a directional change was specified.

https://doi.org/10.1038/s41591-026-04491-7

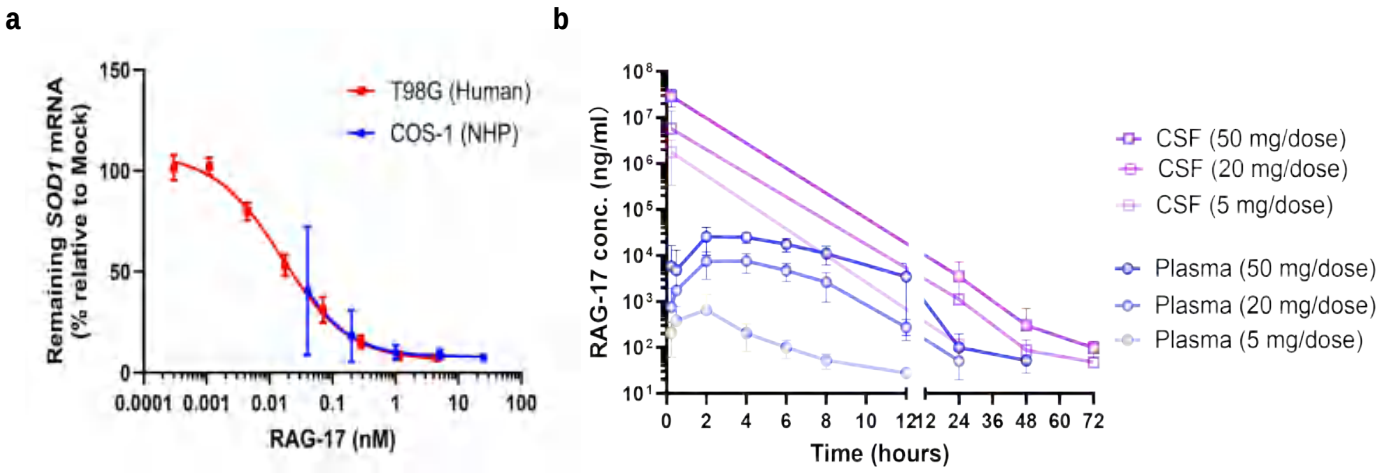

Extended Data Fig. 5 | In vitro RAG-17 cross-species activity and PK in cynomolgus monkeys. a, Cross-species activity. In silico analysis using https://genome.ucsc.edu/ to identify mismatches between *SOD1* transcripts of different species and the 'seed' region of the RAG-17 guide strand. Species-specific cell lines-T98G (human) and COS-1 (green monkey) were transfected with RAG-17 at multiple concentrations for 24 h and species-specific *SOD1* mRNA expression was assayed by RT-qPCR. **b**, PK in cynomolgus monkeys. CSF and plasma were collected from monkeys administered RAG-17 (5, 20, or 50 mg/dose) via IT injection. Samples were collected at predose, 15 min, 24 h, 48 h and 72 h (CSF and plasma) and additionally at 2 h, 4 h, 6 h, 8 h, and 12 h (plasma only) postdose. RAG-17 concentrations were analyzed by validated LC–MS/MS methods. Each group included 10 animals (5 males and 5 females). Data represent mean ± s.d.

https://doi.org/10.1038/s41591-026-04491-7

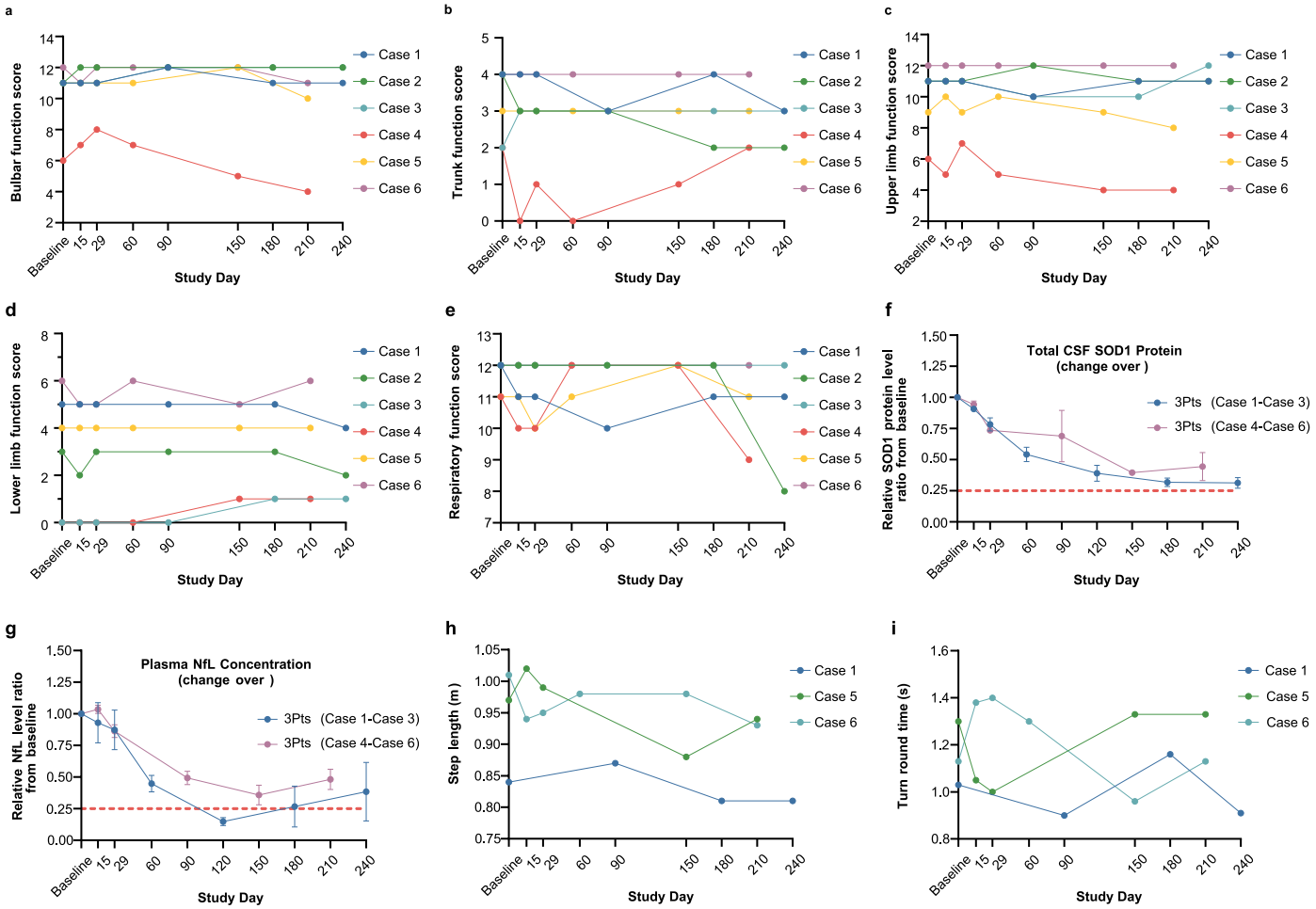

Extended Data Fig. 6 | Preliminary Efficacy of RAG-17 in human patients. **a**–**e**, Longitudinal changes in ALSFRS-R scores across different functional domains: bulbar function (**a**), trunk function (**b**), upper limb function (**c**), lower limb function (**d**), and respiratory (**e**). **f**, CSF SOD1 protein levels presented as a group summary. Bars represent mean ± s.e.m. **g**, Plasma NfL levels presented as a group summary in five patients, with the exclusion of case 1. Bars represent mean ± s.e.m. **h**,**i**, Gait function assessed by three-dimensional gait analysis under multitasks (including step length (**h**) and turn round time (**i**)). The horizontal dashed line in the background (**f** and **g**) represents a reference threshold at 25% of the baseline SOD1 (**f**) or NfL (**g**) level, indicating the point at which the concentration has fallen to one quarter of the starting value.

nature portfolio

Corresponding author(s): Yilong Wang

Last updated by author(s): May 20, 2026

Reporting Summary

Nature Portfolio wishes to improve the reproducibility of the work that we publish. This form provides structure for consistency and transparency in reporting. For further information on Nature Portfolio policies, see our Editorial Policies and the Editorial Policy Checklist.

Statistics

For all statistical analyses, confirm that the following items are present in the figure legend, table legend, main text, or Methods section.

n/a	Confirmed
☐	☒ The exact sample size (*n*) for each experimental group/condition, given as a discrete number and unit of measurement
☐	☒ A statement on whether measurements were taken from distinct samples or whether the same sample was measured repeatedly
☐	☒ The statistical test(s) used AND whether they are one- or two-sided *Only common tests should be described solely by name; describe more complex techniques in the Methods section.*
☒	☐ A description of all covariates tested
☒	☐ A description of any assumptions or corrections, such as tests of normality and adjustment for multiple comparisons
☐	☒ A full description of the statistical parameters including central tendency (e.g. means) or other basic estimates (e.g. regression coefficient) AND variation (e.g. standard deviation) or associated estimates of uncertainty (e.g. confidence intervals)
☐	☒ For null hypothesis testing, the test statistic (e.g. *F*, *t*, *r*) with confidence intervals, effect sizes, degrees of freedom and *P* value noted *Give P values as exact values whenever suitable.*
☒	☐ For Bayesian analysis, information on the choice of priors and Markov chain Monte Carlo settings
☒	☐ For hierarchical and complex designs, identification of the appropriate level for tests and full reporting of outcomes
☒	☐ Estimates of effect sizes (e.g. Cohen's *d*, Pearson's *r*), indicating how they were calculated

Our web collection on statistics for biologists contains articles on many of the points above.

Software and code

Policy information about availability of computer code

Data collection	For pre-clinical data, raw instrument data were acquired using dedicated vendor software: 480 Real-Time PCR system (Roche) for Real-Time PCR experiments, and Analyst™ Software (Thermo Fisher) for LC-MS/MS bioanalysis. Other experimental metadata were recorded by common softwares. Clinical data with all case information were managed using an electronic data capture system (eCRF).
Data analysis	In silico alignment algorithm from gggenome (https://gggenome.dbcls.jp), miRanda (Rick Masonbrink), GraphPad Prism version 8.3.0, Watson LIMS (Certara), SAS software (V.9.4, SAS Institute).

For manuscripts utilizing custom algorithms or software that are central to the research but not yet described in published literature, software must be made available to editors and reviewers. We strongly encourage code deposition in a community repository (e.g. GitHub). See the Nature Portfolio guidelines for submitting code & software for further information.

Data

Policy information about availability of data

All manuscripts must include a data availability statement. This statement should provide the following information, where applicable:

- Accession codes, unique identifiers, or web links for publicly available datasets
- A description of any restrictions on data availability
- For clinical datasets or third party data, please ensure that the statement adheres to our policy

All primary data supporting the findings of this study are included in this article and its supplementary files. Individual de-identified participant data that support the

findings of this study are not publicly available due to privacy and ethical restrictions. These data are stored on the secure server of the China National Clinical Research Center for Neurological Diseases and can be accessed under controlled access to verify the research conclusions. Access to these data is granted to qualified researchers following a review and approval process managed by the center's data access committee. Researchers who provide an methodologically sound analysis proposal that complies with clinical study ethical and data integrity requirements can request access via the center's Data Management and Sharing System (https://paper.ncrcnd.org.cn) or by contacting the corresponding author Y.W (yilong528@aliyun.com). Requests will be evaluated within 30 days. The study protocol and statistical analysis plan are available in the Supplementary Information_Protocol and Supplementary Information_SAP.

Research involving human participants, their data, or biological material

Policy information about studies with human participants or human data. See also policy information about sex, gender (identity/presentation), and sexual orientation and race, ethnicity and racism.

Reporting on sex and gender	All participants provided informed consent prior to screening. Eligible patients (both men and women) were aged 18 to 75 years. Sex or gender information was collected based on self-reporting and recorded within the electronic case report form (eCRF). No sex/gender-based subgroup analysis was performed, because the study objectives were designed independently of sex or gender.
Reporting on race, ethnicity, or other socially relevant groupings	None of these categorization variables was used.
Population characteristics	Relevant population characteristics of the human research participants are the following: All six enrolled participants carried a confirmed pathogenic or likely pathogenic SOD1 mutation associated with ALS. Median age was 47 years (range 26–67). Four female and two male patients were included. Detailed baseline characteristics are provided in Table 1.
Recruitment	Participants were identified by review of the medical records / clinic database held within the institution, and direct physician referral. Patients with a confirmed diagnosis of amyotrophic lateral sclerosis (ALS) and carrying a pathogenic or likely pathogenic SOD1 mutation were assessed for eligibility. Complete inclusion and exclusion criteria are listed both in the main manuscript (Methods section) and in the full study protocol, provided in the Supplementary Information. All patients were recruited from clinical site in China. Potential referral bias (physicians may refer more severe phenotypes) and self□selection bias (if eligible patients declined). Single□site design limits generalisability.
Ethics oversight	This study was approved by the ethics committee of Beijing Tiantan Hospital (ethical approval No. KY2023-015-02). Written informed consent was obtained from all participants prior to any study-related procedures, in accordance with the Declaration of Helsinki and Good Clinical Practice guidelines. Participants received a fixed travel allowance and a modest reimbursement for blood and cerebrospinal fluid collection procedures. No other compensation was provided for study participation.

Note that full information on the approval of the study protocol must also be provided in the manuscript.

Field-specific reporting

Please select the one below that is the best fit for your research. If you are not sure, read the appropriate sections before making your selection.

☒ Life sciences ☐ Behavioural & social sciences ☐ Ecological, evolutionary & environmental sciences

For a reference copy of the document with all sections, see nature.com/documents/nr-reporting-summary-flat.pdf

Life sciences study design

All studies must disclose on these points even when the disclosure is negative.

Sample size	i)Pre-clinical study: The sample sizes for the efficacy studies in SOD1G93A mice (n=10-11/group) and rats (n=11-20/group), and the pharmacodynamic study in cynomolgus monkeys (n=10/group, balanced by sex), were determined based on standard practices in the field for such models and endpoints. These sizes were deemed sufficient to robustly assess treatment effects and safety signals to support translation to clinical trials. No statistical methods were used to determine sample size. ii)Clinical study: This was a first-in-human, single-arm, open-label study designed primarily to evaluate the safety, tolerability, pharmacokinetics (PK), and preliminary bioactivity of RAG-17 in patients with SOD1-ALS. A total of six participants were enrolled. No formal power calculation was performed for this early-phase study. This sample size was considered sufficient for an initial proof-of-concept study to inform future trial design, based on the rarity of the patient population (SOD1-ALS), clinical feasibility, and the magnitude of target engagement (SOD1 reduction).
Data exclusions	i)Pre-clinical study: Animals that developed severe health issues unrelated to the expected ALS disease progression were excluded from the final analysis. These pre-defined criteria ensured that the assessment of treatment efficacy was not confounded by unrelated morbidity. ii)Clinical study: All six enrolled participants received the intended dose of RAG-17 and were included in both the safety and efficacy analyses; no patients were excluded. However, not all planned exploratory assessments were completed for every patient due to an inability to comply with specific procedures (e.g., gait function) as a result of disease progression. All available data were analyzed and reported as specified in the protocol.
Replication	i)Pre-clinical study: Statistical analysis demonstrated significant and consistent treatment effects across key in-life (e.g., grip strength, rotarod) and post-mortem (e.g., SOD1 quantification) endpoints. Experimental findings were supported by appropriate biological and technical replicates within the study. Individual animal-level source data are not included in the manuscript but are archived by the authors and

available for verification upon reasonable request.
ii)Clinical study: This single-arm, open-label, first-in-human trial was designed to evaluate safety and preliminary efficacy in a defined patient population (SOD1-ALS). As such, no applicable replication validation is provided.

Randomization

i)Pre-clinical study: SOD1 transgenic animals and their wild-type littermates were randomly assigned to experimental groups based on body weight and sex to ensure balanced distribution across all groups.
ii)Clinical study: This is a single-arm, open-label study. No randomization was applied.

Blinding

i)Pre-clinical study: The following analyses were conducted in a blinded fashion: neurological scoring, grip strength test, rotarod test, RNAscope in situ hybridization, tissue distribution and quantification of RAG-17 in rats, SOD1 mRNA and protein expression in cynomolgus monkey CNS, as well as histopathological staining. For these analyses, the investigators were unaware of the treatment group assignment until after all data were collected and analyzed.
ii)Clinical study: Blinding was not applied since this is a single-arm, open-label study. All participants were aware of the treatment they received, and the investigators were not blinded to treatment allocation.

Reporting for specific materials, systems and methods

We require information from authors about some types of materials, experimental systems and methods used in many studies. Here, indicate whether each material, system or method listed is relevant to your study. If you are not sure if a list item applies to your research, read the appropriate section before selecting a response.

Materials & experimental systems

n/a	Involved in the study
☐	☒ Antibodies
☐	☒ Eukaryotic cell lines
☒	☐ Palaeontology and archaeology
☐	☒ Animals and other organisms
☐	☒ Clinical data
☒	☐ Dual use research of concern
☒	☐ Plants

Methods

n/a	Involved in the study
☒	☐ ChIP-seq
☒	☐ Flow cytometry
☐	☒ MRI-based neuroimaging

Antibodies

Antibodies used

Anti-Choline Acetyltransferase Antibody (Merck Millipore, Cat.No.AB144P, Lot No. 4145737), Peroxidase AffiniPure™ Donkey Anti-Goat IgG (H+L) Polyclonal Antibody (JacksonImmunoResearch, Cat.No.705-035-003, Lot No. 161760).

Validation

Anti-Choline Acetyltransferase Antibody (AB144P): Validation data provided by the manufacturer (Merck Millipore) indicates specificity for human, opossum, guinea pig, rat, mouse, zebrafish, avian, monkey, chicken Choline Acetyltransferase by WB, ICC and IHC. This antibody was also validated in our laboratory using tissue from SOD1G93A rats. Peroxidase AffiniPure™ Donkey Anti-Goat IgG (H+L) (705-035-003) Validation data provided by the manufacturer (JacksonImmunoResearch). The secondary antibodies were used according to the manufacturer's recommendations.

Eukaryotic cell lines

Policy information about cell lines and Sex and Gender in Research

Cell line source(s)

T98G cells were obtained from Cobioer (Catalog # CBP60301). COS-1 cells were obtained from ATCC (Catalog# CRL-1650). RK13 cells were obtained from ATCC (Catalog# CCL-37). MB-49 cells were obtained from Millipore Sigma (Catalog# SCC148). C6 cells were obtained from Amyjet (Catalog# BNCC100216).

Authentication

All cell lines were obtained directly from the indicated commercial suppliers. No additional cell line authentication (e.g., STR profiling) was performed by the authors.

Mycoplasma contamination

Cells were not routinely tested for mycoplasma contamination during this study.

Commonly misidentified lines
(See ICLAC register)

We did not use any misidentified cell line in this study.

Animals and other research organisms

Policy information about studies involving animals; ARRIVE guidelines recommended for reporting animal research, and Sex and Gender in Research

Laboratory animals

Female and male cynomolgus monkeys (age, approximately 3.0-4.0 years; body weights, 2.2-3.2 kg for females and 2.4-4.4 kg for males) were obtained from Guang Dong Blooming-Spring Biological Technology Development Co., Ltd. hSOD1G93A mice (B6. Cg-Tg (SOD1*G93A)1Gur/J) (Strain ID #004435) were obtained from the Jackson Laboratory. SOD1G93A transgenic rats were obtained from

	Taconic Biosciences (model 2148).
Wild animals	This study did not involve wild animals.
Reporting on sex	Female hSOD1G93A mice, female and male SOD1G93A transgenic rats as well as female and male cynomolgus monkeys were used.
Field-collected samples	This study did not involve samples collected from the field.
Ethics oversight	All procedures and any amendments or procedures involving the care or use of animals in this study were reviewed and approved by the Institutional Animal Care and Use Committee of Nantong University (#S20220323-001), WuXi AppTtec (#GP02-QD105-2020V1.0, H59-0027-TX), prior to the initiation of these procedures.

Note that full information on the approval of the study protocol must also be provided in the manuscript.

Clinical data

Policy information about clinical studies

All manuscripts should comply with the ICMJE guidelines for publication of clinical research and a completed CONSORT checklist must be included with all submissions.

Clinical trial registration	NCT05903690
Study protocol	Study protocol available as supplementary material, along with the statistical analysis plan.
Data collection	Between 22 May, 2023, and 27 November, 2023, a total of seven individuals were screened. One individual did not met the inclusion criteria and was excluded, resulting in six being successfully enrolled. All six enrolled participants received treatment with RAG-17 and underwent clinical assessment at Beijing Tiantan Hospital, Capital Medical University. The data collection period spanned from 24 May, 2023, to 11 July, 2024. Clinical data were collected using individual case report forms (CRFs) by study physicians, with all case information managed using an electronic data capture system (eCRF).
Outcomes	i)The primary endpoints included the following safety evaluation measures: 1) incidence of adverse events (AEs) and serious adverse events (SAEs) within 240 days after RAG-17 treatment; 2) changes in laboratory assessments, vital signs, ALS Functional Rating Scale-Revised (ALSFRS-R) scores, and abnormalities in heart, lung and abdomen examinations, neurological examinations, as well as electrocardiograms within 240 days after the first injection of RAG-17. The ALSFRS-R consists of 12 items across four subdomains of bodily function (bulbar, fine motor, gross motor, and breathing). Each item is scored on an ordinal scale from 0 (total loss of function) to 4 (no loss of function), yielding total scores ranging from 0 to 48, with higher scores indicating better function. ii)The secondary endpoints included: (1) changes in CSF SOD1 protein levels at days 15, 29, 60, 120, 180 and 240 from baseline; (2) changes in plasma NfL levels at days 1, 15, 29, 60, 120, 180 and 240 from baseline; (3) pharmacokinetics of RAG-17 in plasma at days 1, 15, 29, 60, 120, 180 and 240; and (4) time to invasive mechanical ventilation or death. iii)The exploratory endpoints included changes in: (1-7) pulmonary function (including FVC), fatigue severity, muscle strength, gait function, modified Norris scale scores, quality of life and clinical staging, at days 15, 29, 90, 180 and 240; and (8-9) electromyography and 7T MRI imaging features at days 29, 90, 180 and 240. Fatigue severity was assessed using the Fatigue Severity Scale (FSS)40. Evaluation of gait function included 3D gait analysis, short physical performance battery, tandem walking, and the 6-meter walk test. Quality of life was estimated using the Amyotrophic Lateral Sclerosis Assessment Questionnaire 40 (ALSAQ-40), a Five-level version of EuroQol Five Dimensions Questionnaire (EQ-5D-5L), Hamilton Anxiety Scale (HAMA) and Hamilton Depression Scale (HAMD). Clinical staging was evaluated using the London ALS Stage and Milano-Torino staging. The electromyographic features evaluated in this study included the composite muscle action potentials (CMAP), motor unit number index (MUNIX), and motor unit size index (MUSIX).

Plants

Seed stocks	Not applicable.
Novel plant genotypes	Not applicable.
Authentication	Not applicable.

Magnetic resonance imaging

Experimental design

Design type	Structural MRI of the human brain in vivo.
Design specifications	Whole-brain three-dimensional T1-weighted imaging (T1WI) and three-dimensional SWI.

Behavioral performance measures: Not performed.

Acquisition

Imaging type(s): 3D T1-weighted MP2RAGE and 3D SWI.

Field strength: 7.0 Tesla

Sequence & imaging parameters: T1WI (MP2RAGE): sagittal 3D scan, TE/TR/TI1/TI2=3.27/4500/1000/3200ms, slices=240, voxel size=0.8×0.8×0.8mm3; SWI: axial 3D scan, TE/TR=12/19ms, slices=104, voxel size=0.3×0.3×1.2mm3.

Area of acquisition: Whole brain.

Diffusion MRI ☐ Used ☒ Not used

Preprocessing

Preprocessing software: None used.

Normalization: Not performed.

Normalization template: Not performed.

Noise and artifact removal: Not performed.

Volume censoring: Not performed.

Statistical modeling & inference

Model type and settings: Not applicable.

Effect(s) tested: Not applicable.

Specify type of analysis: ☒ Whole brain ☐ ROI-based ☐ Both

Statistic type for inference: Not applicable.

(See Eklund et al. 2016)

Correction: Not applicable.

Models & analysis

n/a	Involved in the study
☒	☐ Functional and/or effective connectivity
☒	☐ Graph analysis
☒	☐ Multivariate modeling or predictive analysis